Coordination Chemistry and Reactivity of New Zwitterionic Rhodium and Iridium Complexes Featuring the Tripodal Phosphine Ligand $[PhB(CH_2P^iPr_2)_3]^-$. Activation of H−H, Si−H, and Ligand B−C Bonds

Laura Turculet, Jay D. Feldman, and T. Don Tilley*

Department of Chemistry, University of California at Berkeley, Berkeley, California 94720-1460

Received December 15, 2003

The synthesis, characterization, and reactivity of zwitterionic rhodium and iridium complexes containing the tris(phosphino)borate ligand $[PhB(CH_2P^iPr_2)_3]^-$ ($[PhBP_3']^-$) are reported. The allyl complexes $[PhBP_3']IrH(\eta^3\text{-}C_8H_{13})$ (**3**) and $[PhBP_3']IrH(\eta^3\text{-}C_3H_5)$ (**4**) were prepared by reaction of $[PhBP_3']Li(THF)$ (**2**) with the corresponding $[(alkene)_2IrCl]_2$ complex. Complex **3** reacted with secondary silanes (H_2SiR_2, with R = Et, Ph) to give silyl-capped trihydride complexes of the type $[PhBP_3']IrH_3(SiHR_2)$ (R = Et, **5**; Ph, **6**) with concomitant β-hydride elimination of 1,3-cyclooctadiene. Complex **5** underwent H/D exchange with D_2 to incorporate deuterium into both the Ir−H and Si−H positions. The reaction of **5** with 1 equiv of PMe_3 resulted in elimination of Et_2SiH_2 to form the corresponding dihydride complex, $[PhBP_3']Ir(H)_2(PMe_3)$ (**7**). Complexes of the type $[PhBP_3']Ir(H)_2(L)$ (L = PMe_3, **7**; PH_2Cy, **8**; CO, **9**) could also be prepared directly by the reaction of **3** with L. The observed reactivity of $[PhBP_3']Ir$ complexes is compared with that of the related $[PhB(CH_2PPh_2)_3]^-$ ($[PhBP_3]^-$) species. The Rh(I) complexes $[\kappa^2\text{-}PhBP_3']Rh(PMe_3)_2$ (**10**) and $[PhBP_3']Rh(CO)_2$ (**11**) are also reported. Variable-temperature ^1H and ^{31}P NMR experiments did not reveal evidence for $\kappa^2-\kappa^3$ interconversion for **10** and **11**. However at elevated temperatures **10** was found to engage in a dynamic equilibrium process involving dissociation of the PMe_3 ligands and reversible migration of a $-CH_2$ group in the ligand backbone from B to Rh. The product of this migration, $[PhB(CH_2P^iPr_2)_2]\overline{RhCH_2P^iPr_2}$ (**12**), was prepared independently by the reaction of **2** with $[RhCl(C_2H_4)_2]_2$ and was structurally characterized by X-ray crystallography. Complex **10** reacted with H_2 to give the oxidative addition product $[PhBP_3']Rh(H)_2(PMe_3)$ (**13**). The reaction of **10** with 1 equiv of Ph_2SiH_2 resulted in loss of a ligand arm to give the bis(phosphino)borane complex $[PhB(CH_2P^iPr_2)_2]Rh(H)_2(SiHPh_2)(PMe_3)$ (**14**). Complex **11** reacted with H_2 in the presence of 1 equiv of Me_3NO to give the oxidative addition product $[PhBP_3']Rh(H)_2(CO)$ (**15**), with concomitant liberation of Me_3N.

Introduction

The controlled activation of element−hydrogen bonds by transition metal complexes represents a fundamental step in a number of metal-catalyzed transformations.[1] In particular, the activation of Si−H bonds by metal fragments has been shown to be a key component of olefin hydrosilylation and dehydrogenative silylation processes, as well as in the dehydrocoupling of hydrosilanes to polysilanes.[2] For late transition metal complexes, these bond activations generally involve the oxidative addition of Si−H bonds to the metal center; however, considerable attention has focused on determining the extent to which further rearrangements of the resulting metal silyl species may contribute to the observed transformations.[2]

Along these lines, research in our group has focused on elucidating the chemistry of transition metal-mediated Si−H bond activation processes. Recently, we reported the first direct observations of 1,2-hydride shifts (α-eliminations) that convert transition metal silyl complexes into base-free metal silylene hydrides.[3] Given the relative scarcity of isolable base-free metal silylene complexes,[2−4] as well as their potential to mediate new

(1) Elschenbrioch, C.; Salzer, A. *Organometallics: A Concise Introduction, Second Edition*; VCH: New York, 1992; Chapter 17, p 411.

(2) (a) Tilley, T. D. In *The Chemistry of Organic Silicon Compounds*; Patai, S., Rappoport, Z., Eds.; Wiley: New York, 1989; Chapter 24, p 1415. (b) Ojima, I. In *The Chemistry of Organic Silicon Compounds*; Patai, S., Rappoport, Z., Eds.; Wiley: New York, 1989; Chapter 25, p 1479. (c) Tilley, T. D. *Comments Inorg. Chem.* **1990**, *10*, 37. (d) Tilley, T. D. In *The Silicon-Heteroatom Bond*; Patai, S., Rappoport, Z., Eds.; Wiley: New York, 1991; Chapters 9 and 10, pp 245−309. (e) Pannell, K. H.; Sharma, H. *Chem. Rev.* **1995**, *95*, 1351. (f) Eisen, M. S. In *The Chemistry of Organic Silicon Compounds, Volume 2*; Apeloig, Y., Rappoport, Z., Eds.; Wiley: New York, 1998; Chapter 35, p 2037. (g) Corey, J. Y.; Braddock-Wilking, J. *Chem. Rev.* **1999**, *99*, 175.

(3) For examples of transition metal silylene complexes prepared via α-hydride elimination routes, see: (a) Mitchell, G. P.; Tilley, T. D. *J. Am. Chem. Soc.* **1998**, *120*, 7635. (b) Mitchell, G. P.; Tilley, T. D. *Angew. Chem., Int. Ed.* **1998**, *37*, 2524. (c) Peters, J. C.; Feldman, J. D.; Tilley, T. D. *J. Am. Chem. Soc.* **1999**, *121*, 9871. (d) Klei, S. R.; Tilley, T. D.; Bergman, R. G. *J. Am. Chem. Soc.* **2000**, *122*, 1816. (e) Mork, B. V.; Tilley, T. D. *J. Am. Chem. Soc.* **2001**, *123*, 9702. (f) Feldman, J. D.; Peters, J. C.; Tilley, T. D. *Organometallics* **2002**, *21*, 4065.

10.1021/om030686e CCC: $27.50
Publication on Web 04/07/2004

chemical transformations, we have sought to develop reaction systems for which this α-hydride elimination process is facile. In this context, we have previously introduced the anionic, tripodal phosphino-borate ligand $[PhB(CH_2PPh_2)_3]^-$ ($[PhBP_3]^-$) and demonstrated its utility in facilitating the preparation of zwitterionic, base-free, iridium silylene and germylene complexes via the sequential activation of two E−H (E = Si, Ge) fragments on a single R_2EH_2 substrate (eq 1).[3c,f] This silylene extrusion reaction appears to involve 1,2-hydride migrations between iridium and silicon and is exceptional in that the direct conversion of secondary silanes to silylene complexes was previously unknown.

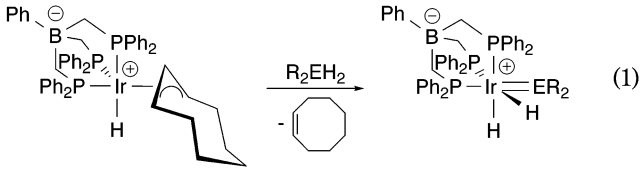

(1)

The reactivity observed in our initial study of iridium complexes featuring the $[PhBP_3]^-$ ligand prompted us to further examine the chemistry of this system and of related metal species. One area of interest concerns delineation of the steric and electronic factors that influence reactivity in such phosphino-borate complexes. In particular, we are interested in studying the effects of a more electron-donating phosphino-borate ligand on the bond activation chemistry of the corresponding iridium complexes, as strongly electron-donating ligands have been shown to promote transition metal-mediated chemical transformations that are not accessible to less electron-rich complexes.[5] Additionally, our synthetic and mechanistic investigations have revealed that the phenyl substituents on the phosphine donors of the $[PhBP_3]^-$ ligand are susceptible to intramolecular *ortho*-metalation by the iridium center.[3f,6] We therefore became interested in replacing these phenyl groups with more metalation-resistant substituents that would disfavor such ligand activation processes.

In the pursuit of a more electron-donating and metalation-resistant analogue of $[PhBP_3]^-$, we recently detailed the preparation of $[PhB(CH_2P^iPr_2)_3]Li(THF)$ ($[PhBP_3']Li(THF)$, **2**; eq 2).[7] Preliminary work in our

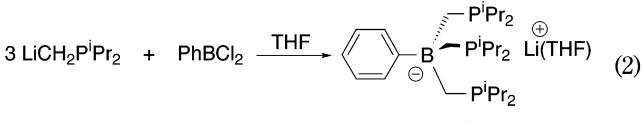

(2)

Scheme 1

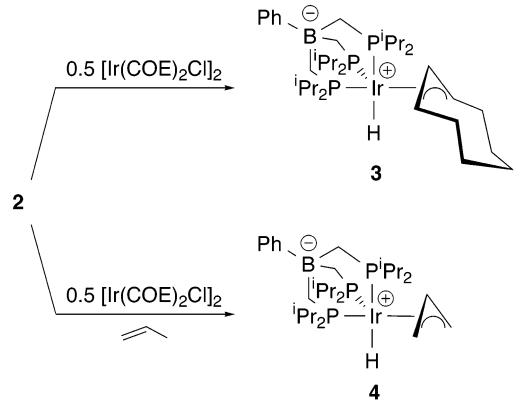

laboratory has demonstrated that **2** is an effective transfer reagent for the $[PhBP_3']^-$ ligand, which can be used in the synthesis of unusual four-ccordinate $[PhBP_3']$-Fe(II) silyl complexes.[7] Additionally, Peters and co-workers have recently reported the synthesis of $[PhBP_3']Tl$ and demonstrated novel dinitrogen activation chemistry involving $[PhBP_3']Fe$ and $[PhBP_3']Co$ complexes.[8] In this contribution, we extend this chemistry to the synthesis and bond activation reactivity of iridium complexes supported by $[PhBP_3']^-$. We also report for the first time the synthesis and chemical reactivity of several rhodium complexes featuring tris(phosphino)borate ligation.

Results and Discussion

Synthesis of $[PhBP_3']Ir$ Allyl Complexes. The reaction of the salt $[PhB(CH_2P^iPr_2)_3]Li(THF)$ (**2**) with $[(COE)_2IrCl]_2$ (COE = cyclooctene) provided high-yield entry to the chemistry of $[PhBP_3']Ir$. This reaction occurred readily at room temperature in benzene solvent to give zwitterionic $[PhBP_3']IrH(\eta^3\text{-}C_8H_{13})$ (**3**) via C−H activation of a COE ligand (Scheme 1). The formation of **3** was quantitative within 10 min by ^1H NMR and ^{31}P NMR spectroscopy (benzene-d_6), and the product was isolated in >90% yield. This transformation is analogous to that used to prepare $[PhBP_3]IrH(\eta^3\text{-}C_8H_{13})$ (**1**),[3c,6] as well as the hydridotris(pyrazolyl)borate (Tp) analogue, $TpIrH(\eta^3\text{-}C_8H_{13})$.[9] Unlike the preparation of **1**, however, no evidence for the formation of side-products other than cyclooctene and lithium chloride was observed, and the reaction mixture maintained a golden orange color.

Complex **3** exhibits spectroscopic characteristics consistent with the structure shown in Scheme 1. The $^{31}P\{^1H\}$ NMR spectrum of **3** (benzene-d_6) contains a doublet at 7.52 ppm ($^2J_{PP}$ = 21 Hz) and a triplet at −18.08 ppm ($^2J_{PP}$ = 21 Hz) in a 2:1 ratio, consistent with a mirror plane of symmetry that bisects the $[PhBP_3']$ ligand. The ^1H NMR spectrum of **3** (benzene-d_6) is significantly complicated by a large number of overlapping, intense resonances in the alkyl region of the spectrum (2.5−0.5 ppm) due to the ligand P-isopropyl substituents. However, several diagnostic features of the spectrum

(4) For additional examples of base-free transition metal dialkyl and diaryl silylene complexes prepared by routes other than α-hydride elimination, see: (a) Grumbine, S. K.; Mitchell, G. P.; Straus, D. A.; Tilley, T. D.; Rheingold, A. L. *Organometallics* **1998**, *17*, 5607. (b) Wanandi, P. W.; Glaser, P. B.; Tilley, T. D. *J. Am. Chem. Soc.* **2000**, *122*, 972. (c) Feldman, J. D.; Mitchell, G. P.; Nolte, J.-O.; Tilley, T. D. *J. Am. Chem. Soc.* **1998**, *120*, 11184.

(5) Werner, H. *Angew. Chem., Int. Ed. Engl.* **1983**, *22*, 927, and references therein.

(6) Feldman, J. D.; Peters, J. C.; Tilley, T. D. *Organometallics* **2002**, *21*, 4050.

(7) Turculet, L.; Feldman, J. D.; Tilley, T. D. *Organometallics* **2003**, *22*, 4627.

(8) (a) Betley, T. A.; Peters, J. C. *Inorg Chem.* **2003**, *42*, 5074. (b) Betley, T. A.; Peters, J. C. *J. Am. Chem. Soc.* **2003**, *125*, 10782.

(9) (a) Tanke, R. S.; Crabtree, R. H. *Inorg. Chem.* **1989**, *28*, 3444. (b) Fernandez, M. J.; Rodriguez, M. J.; Oro, L. A.; Lahoz, F. J. *J. Chem. Soc., Dalton Trans.* **1989**, 2073. (c) Alvarado, Y.; Boutry, O.; Gutierrez, E.; Monge, A.; Nicasio, M. C.; Poveda, M. L.; Perez, P. J.; Ruiz, C.; Bianchini, C.; Carmona, E. *Chem., Eur. J.* **1997**, *3*, 860.

are evident, such as the allyl methine resonances (multiplets at 5.08 and 3.77 ppm) and an iridium hydride resonance at −15.30 ppm that appears as a doublet of triplets due to large *trans*-phosphine coupling ($^2J_{HPtrans}$ = 120 Hz) and weaker coupling to the *cis*-phosphine donors ($^2J_{HPcis}$ = 17 Hz).

The parent allyl complex [PhBP$_3$′]IrH(η^3-C$_3$H$_5$) (**4**) was obtained by addition of [PhB(CH$_2$P^{i}Pr$_2$)$_3$]Li(THF) to a frozen THF solution of [(COE)$_2$IrCl]$_2$ that had been saturated with propene (Scheme 1). Compound **4** was isolated as an off-white crystalline solid in 67% yield and exhibits spectroscopic characteristics analogous with those of **3**, consistent with a similar structure, as shown in Scheme 1.

Reactions of [PhBP$_3$′]Ir Allyl Complexes with Silanes. Complex **3** reacted with secondary silanes (H$_2$SiR$_2$, with R = Et, Ph) at 65 °C in benzene-d_6 solution to generate 1 equiv of 1,3-COD (COD = cyclooctadiene) and a new Ir−H species, [PhBP$_3$′]IrH$_3$(SiHR$_2$) (eq 3, R = Et, **5**; R = Ph, **6**). The NMR characteristics of **5** and **6** are consistent with the 3-fold symmetric, silyl-capped Ir(V) trihydride structure indicated in eq 3. Both **5** and

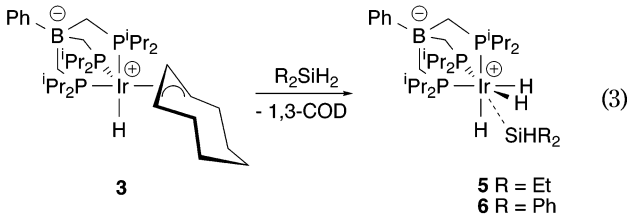

3 **5** R = Et, **6** R = Ph (3)

6 exhibit only one ^{31}P{^{1}H} NMR resonance, observed at 7.53 and 7.85 ppm, respectively (benzene-d_6, room temperature). By ^{1}H NMR spectroscopy, both complexes exhibit an Ir−H resonance that integrates as three hydrogens (for **5**: −12.27 ppm, $^2J_{HP}$ = 65 Hz; for **6**: −11.55 ppm, $^2J_{HP}$ = 53 Hz), as well as an Si−H resonance (for **5**: 5.78 ppm, $^1J_{SiH}$ = 193 Hz; for **6**: 5.71 ppm, $^1J_{SiH}$ = 245 Hz) that integrates as one hydrogen. The ^{29}Si NMR spectra for **5** and **6** contain a quartet at −19.8 ppm ($^2J_{SiP}$ = 5 Hz) and −23.9 ppm ($^2J_{SiP}$ = 7 Hz), respectively, consistent with coupling to three equivalent phosphorus nuclei. This reaction was quantitative by ^{1}H and ^{31}P NMR spectroscopy, and both complexes were isolated in >90% yield. When the more sterically hindered silane Mes$_2$SiH$_2$ (Mes = 2,4,6-Me$_3$C$_6$H$_2$) was reacted with **3**, little reaction of the silane was observed in benzene-d_6 solution at temperatures up to 100 °C. Decomposition of **3** was observed under these conditions, to give 1,3-COD and a mixture of unidentified iridium-containing products.

The solid state structure of **5** was determined by X-ray crystallography and is shown in Figure 1. Selected bond lengths and angles are summarized in Table 1. The Si atom is disordered over two positions, as is one of the ethyl groups on silicon. All P−Ir−P angles are approximately 90°, while the P−Ir−Si angles range from 118° to 130°. Overall, the coordination geometry at iridium is similar to that of the related complexes [PhBP$_3$]IrH$_3$(SiMe$_3$)[3c] and Tp^{Me2}IrH$_3$(SiEt$_3$)[10,11] (Tp^{Me2} = hydridotris(3,5-dimethylpyrazolyl)borate).

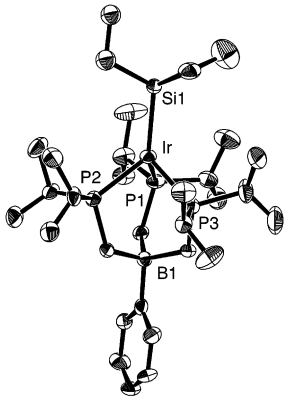

Figure 1. Crystallographically determined structure of [PhB(CH$_2$P^{i}Pr$_2$)$_3$]IrH$_3$(SiHEt$_2$) (**5**) depicted with 50% thermal ellipsoids; all hydrogen atoms have been omitted for clarity.

Table 1. Selected Bond Distances (Å) and Angles (deg) for 5

(a) Bond Distances			
Ir−P1	2.382(2)	Ir−P3	2.376(2)
Ir−P2	2.366(2)	Ir−Si1	2.413(3)
(b) Bond Angles			
P1−Ir−P2	90.89(7)	P1−Ir−Si1	118.42(10)
P1−Ir−P3	89.13(7)	P2−Ir−Si1	129.72(9)
P2−Ir−P3	90.70(7)	P3−Ir−Si1	126.56(8)

The observed reactivity of **3** with H$_2$SiPh$_2$ and H$_2$SiEt$_2$ is surprisingly different from that observed for the analogous complex [PhBP$_3$]IrH(η^3-C$_8$H$_{13}$) (**1**), which reacted with secondary silanes (H$_2$SiR$_2$, with R = Mes, Ph, Et, Me) to generate 1 equiv of COE and the corresponding silylene dihydride complexes, [PhBP$_3$]Ir(H)$_2$(=SiR$_2$) (eq 1).[3c,f] On the basis of the observation of 1,3-COD as a byproduct in the reaction of **3** with silanes, we postulate a mechanism involving β-hydride elimination, which can occur either from the η^1-allyl complex **I** (Scheme 2, path A) or alternatively from **III**, the product of Si−H oxidative addition to **I** (Scheme 2, path B). The former mechanistic path would generate an unsaturated 16 e$^-$ dihydride species "[PhBP$_3$′]Ir(H)$_2$" (**II**), which could then oxidatively add an Si−H bond to give the observed iridium silyl products (Scheme 2, path A). Elimination of 1,3-COD from **III** would require that an open metal coordination site become available, which could occur via dissociation of a ligand arm, for example. By comparison, the reaction of **1** with secondary silanes proceeded via a path involving reductive elimination of COE, which can be envisioned to occur via two possible mechanisms (Scheme 2, paths B and C). One possibility involves reductive elimination of COE from the Ir(III) η^1-allyl complex **I** to generate the η^2-COE complex **IV** (Scheme 2, path C). Reaction of **IV** with a silane Si−H bond, followed by loss of COE, would generate the 16-electron silyl intermediate **V**, which could then undergo 1,2-hydride migration to form the observed silylene

(10) Gutierrez-Puebla, E.; Monge, A.; Paneque, M.; Poveda, M. L.; Taboada, S.; Trujillo, M.; Carmona, E. *J. Am. Chem. Soc.* **1999**, *121*, 346.

(11) A number of group 8 silyl-capped trihydride metal complexes of the type MH$_3$(SiR$_3$)L$_3$ have also been reported. Representative examples include: (a) Knorr, M.; Gilvert, S.; Schubert, U. *J. Organomet. Chem.* **1988**, *347*, C17−C20. (b) Kono, H.; Wakao, N.; Ito, K.; Nagai, Y. *J. Organomet. Chem.* **1977**, *132*, 53. (c) Procopio, L. J.; Berry, D. H. *J. Am. Chem. Soc.* **1991**, *113*, 4039. (d) Buil, M.; Espinet, P.; Esteruelas, M. A.; Lahoz, F. J.; Lledós, A.; Martinez-Ilarduya, J. M.; Maseras, F.; Modrego, J.; Oñate, E.; Oro, L. A.; Sola, E.; Valero, C. *Inorg. Chem.* **1996**, *35*, 1250. (e) Rickard, C. E. F.; Roper, W. R.; Woodgate, S. D.; Wright, L. J. *J. Organomet. Chem.* **2000**, *609*, 177.

Scheme 2

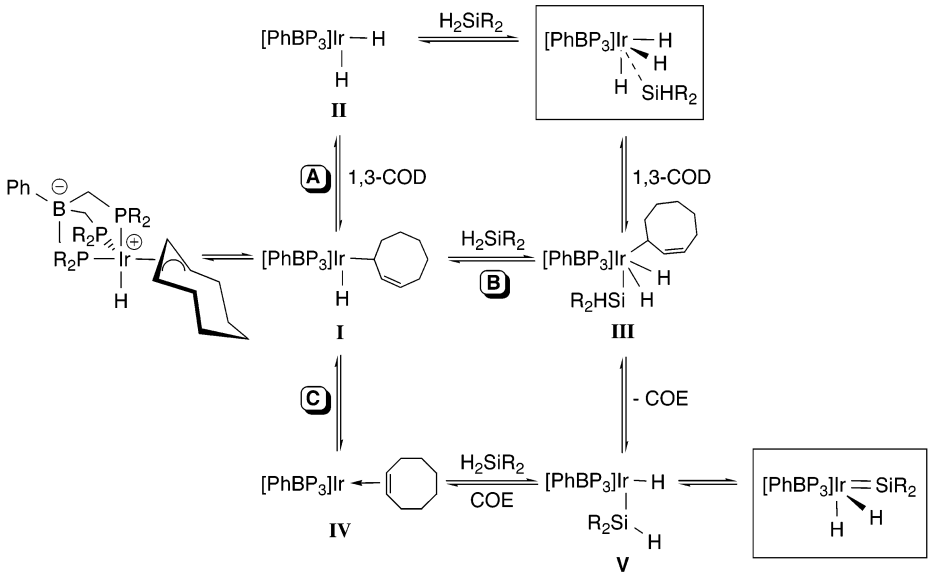

product. Alternatively, as shown in path B, the η^1-allyl complex **I** could oxidatively add a silane Si−H bond to give an Ir(V) intermediate (**III**). Reductive elimination of COE from **III** followed by a 1,2-hydride migration would give the final silylene product. However, these two scenarios are further complicated in the case of **1** by the potential for rapid and reversible intramolecular *ortho*-metalation of the P-phenyl groups on the $PhBP_3$ ligand, which is implied by the facile incorporation of deuterium into the *ortho*-positions of the P-phenyl groups upon reaction of **1** with D_2SiMes_2.[3f]

It is interesting to note that although β-hydride elimination was not observed in the reaction of **1** with secondary silanes, evidence of β-hydride elimination from **1** has been observed under certain other reaction conditions. For example, analogous silyl-capped Ir species $[PhBP_3]IrH_3(SiR_3)$ (R = Et, Me) and 1,3-COD were formed in the reaction of $[PhBP_3]IrH(\eta^3\text{-}C_8H_{13})$ with *tertiary* silanes ($HSiR_3$, where R = Me, Et).[3f] Additionally, $[PhBP_3]Ir(H)_2(PMePh_2)$ was formed, with concomitant loss of 1,3-COD, upon addition of $PMePh_2$ to $[PhBP_3]IrH(\eta^3\text{-}C_8H_{13})$.[6] Thus, while **1** can react via either reductive elimination of COE or β-hydride elimination of 1,3-COD, replacing the P-phenyl substituents with isopropyl groups appears to favor the latter pathway and the formation of silyl-capped iridium trihydride complexes in reactions of **3** with secondary silanes. Reductive elimination from $[PhBP_3']Ir$ complexes may be disfavored as a result of a more electron-rich Ir center relative to the analogous $[PhBP_3]$ complexes.

The related parent allyl complex, **4**, did not react with either Et_2SiH_2 or Ph_2SiH_2 under forcing conditions (benzene-d_6, 100 °C, 5 days). No decomposition of **4** was observed under these reaction conditions. The inertness of **4** is in agreement with the similar lack of reactivity observed for its $[PhBP_3]$ counterpart, $[PhBP_3]IrH(\eta^3\text{-}C_3H_5)$,[3f,6] and may reflect a reduced tendency for the parent allyl ligand to undergo a change in hapticity (η^3 to η^1).

The Si−H resonance observed in the room-temperature ^1H NMR spectrum of the diethylsilyl iridium trihydride complex (**5**) is broad, suggesting the possibility of a fluxional process such as reversible elimination of H_2SiEt_2. This possibility was confirmed by addition of D_2 (1 atm) to a benzene solution of **5**, which resulted in deuterium incorporation into both the Si−H and the Ir−H positions (as indicated by ^2H NMR spectroscopy) after heating at 70 °C over the course of 14 h (eq 4).

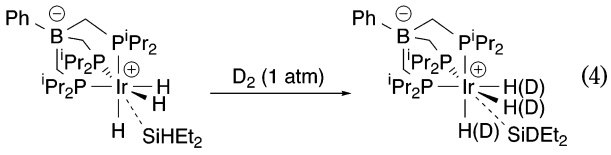

(4)

Elimination of H_2SiEt_2 from **5** was indeed observed upon heating of a benzene-d_6 solution of **3** (90 °C, 20 h) with 1 equiv of PMe_3 (eq 5). This reaction resulted in the

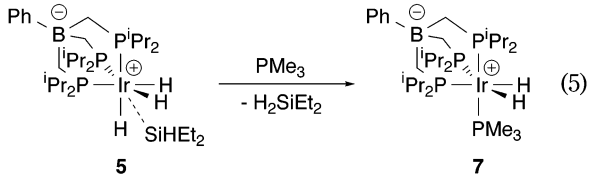

(5)

quantitative formation of 1 equiv of H_2SiEt_2 and the iridium phosphine complex $[PhBP_3']Ir(H)_2(PMe_3)$ (**7**). On the other hand, elimination of H_2 from **5** would lead to the coordinatively unsaturated 16 e^- species $[PhBP_3']IrH(SiHEt_2)$ (**V**), which could then undergo a 1,2-hydride shift from silicon to iridium to generate the corresponding silylene complex, $[PhBP_3']Ir(H)_2(=SiEt_2)$. However, no direct evidence has been observed thus far for reductive elimination of H_2 from **5**. No reaction was observed upon heating of **5** alone or in the presence of 1 equiv of either *tert*-butylethylene or 1-hexene (benzene-d_6, 100 °C, 3 days). Similarly, no reaction was observed upon photolysis of a benzene-d_6 solution of **5** alone or in the presence of 1 equiv of 1-hexene.

Synthesis of $[PhBP_3']Ir(H)_2L$ Complexes (L = PMe_3, PH_2Cy, CO). In keeping with its propensity for β-hydride elimination, compound **3** reacted with a variety of neutral, two-electron-donor ligands to elimi-

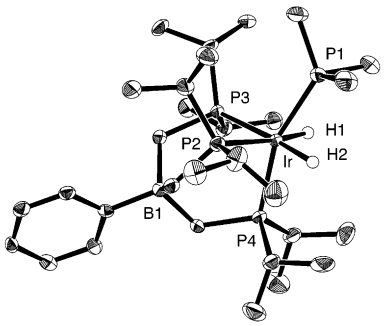

Figure 2. Crystallographically determined structure of $[PhB(CH_2P^iPr_2)_3]Ir(H)_2(PMe_3)\cdot(C_7H_8)_{0.5}$ (**7**·$(C_7H_8)_{0.5}$) depicted with 50% thermal ellipsoids; all hydrogen atoms have been omitted for clarity, with the exception of H1 and H2.

nate 1,3-COD and form complexes of the type $[PhBP_3']Ir(H)_2L$, where L = PMe_3, PH_2Cy, or CO (eq 6). Heating

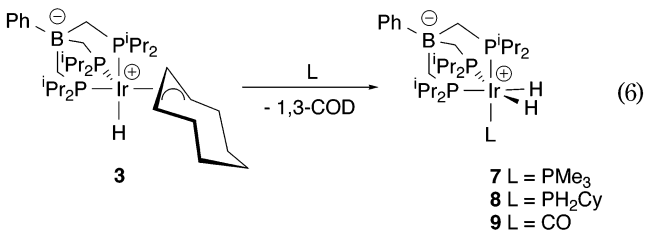

(6)

of a benzene solution of **3** at 65 °C over the course of 16 h in the presence of 1 equiv of either PMe_3 or PH_2Cy resulted in high-yield (>90%) formation of the phosphine complexes $[PhBP_3']Ir(H)_2(PMe_3)$ (**7**) and $[PhBP_3']Ir(H)_2(PH_2Cy)$ (**8**), respectively. The isolated complexes exhibit C_s symmetry in solution, with a mirror plane that contains the iridium center, a phosphorus donor of the $[PhBP_3']$ ligand, and the additional phosphine ligand. Both **7** and **8** contain three sets of resonances in their $^{31}P\{^1H\}$ NMR spectra, consistent with an A_2MX pattern; the two $[PhBP_3']$ phosphorus donors *trans* to hydride ligands are observed as multiplets at −2.15 and −3.24 for **7** and **8**, respectively, while the third $[PhBP_3']$ phosphine arm (doublet of triplets at 15.39 ppm ($^2J_{PPtrans}$ = 286 Hz, $^2J_{PPcis}$ = 21 Hz) for **7** and 16.36 ppm ($^2J_{PPtrans}$ = 284 Hz, $^2J_{PPcis}$ = 20 Hz) for **8**) and the additional phosphine ligand are *trans* to one another (doublet of triplets at −68.15 ppm ($^2J_{PPtrans}$ = 288 Hz, $^2J_{PPcis}$ = 20 Hz) for **7** and a broad doublet at −64.06 ppm ($^2J_{PPtrans}$ = 287 Hz) for **8**). The hydride ligands give rise to a ^1H NMR resonance at −13.50 ppm for **7** and −13.25 ppm for **8** that integrates as two hydrogens for each complex. Heating of benzene-d_6 solutions of either **7** or **8** to 100 °C for up to 5 days did not result in any further reaction. Photolysis of **7** (benzene-d_6, 5 h) also did not lead to any observed reaction.

The solid state structure of **7**·$(C_7H_8)_{0.5}$ was determined by X-ray crystallography and is shown in Figure 2. Selected bond lengths and angles are summarized in Table 2. Both hydride ligands were located, and their positional coordinates were refined. The iridium center exhibits distorted octahedral geometry, with the tripodal phosphine ligand adopting the expected facial coordination featuring P−Ir−P angles of ca. 90°. The PMe_3 ligand is significantly tilted away from the two bulky isopropyl phosphine ligand arms (P1−Ir−P2 and P1−Ir−P3 angles of 101.24(5)° and 105.23(4)°, respectively), giving rise to a P1−Ir−P4 angle of 160.04(5)°. The Ir−P distances reflect the greater *trans* influence of the hydride ligands relative to the phosphine ligands, in that the Ir−P2 and Ir−P3 distances (2.396(1) and 2.376(1) Å, respectively) are longer than the Ir−P1 and Ir−P4 distances (2.303(1) and 2.332(1) Å, respectively).

Table 2. Selected Bond Distances (Å) and Angles (deg) for 7·$(C_7H_8)_{0.5}$

(a) Bond Distances			
Ir−P1	2.303(1)	Ir−P3	2.376(1)
Ir−P2	2.396(1)	Ir−P4	2.332(1)
(b) Bond Angles			
P1−Ir−P2	101.24(5)	P1−Ir−P3	105.23(4)
P2−Ir−P3	89.25(4)	P1−Ir−P4	160.04(5)
P2−Ir−P4	91.56(5)	H1−Ir−P3	80(1)
P3−Ir−P4	90.04(4)	H2−Ir−P2	88(1)

The reaction of CO (1 atm) with **3** in benzene solution at 65 °C resulted in formation of $[PhBP_3']Ir(H)_2(CO)$ (**9**), with the concomitant elimination of 1,3-COD. Compound **9** was isolated in 97% yield and also exhibits C_s symmetry in solution, consistent with a structure similar to that observed for compounds **7** and **8**. An iridium hydride resonance is observed at −11.84 ppm by ^1H NMR spectroscopy (benzene-d_6), and the $^{31}P\{^1H\}$ NMR spectrum contains two resonances in a 1:2 ratio at 11.47 ppm ($[PhBP_3']$ *trans* to CO, $^2J_{PP}$ = 24 Hz) and 3.75 ppm ($[PhBP_3']$ *cis* to CO, $^2J_{PP}$ = 24 Hz), respectively. The IR spectrum of **9** (Nujol mull) contains a characteristic CO stretch at 2003 cm^{-1}. Additional heating of **7** (90 °C, benzene-d_6, 3 days) under an atmosphere of CO did not lead to further reactivity.

Compounds **7**, **8**, and **9** are analogous to the previously reported $[PhBP_3]Ir(H)_2(PMePh_2)$, which was prepared by addition of 1 equiv of $PMePh_2$ to **1**, with similar generation of 1,3-COD.[6] The observation of 1,3-COD suggests that these tris(phosphino)borate-$Ir(H)_2L$ complexes are the products of β-hydride elimination from **3**. Interestingly, the reaction of **1** with 1 equiv of PMe_3 did not lead to formation of the β-hydride elimination product $[PhBP_3]Ir(H)_2(PMe_3)$, but rather to the reductive elimination of COE and formation of $\{PhB[(CH_2PPh_2)_2(CH_2PPhC_6H_4)]\}IrH(PMe_3)$, the product of *ortho*-metalation of a P-phenyl group. This suggests that in the case of **1** ligand activation processes and concomitant COE reductive elimination are competing with a β-hydride elimination pathway.[6] The reaction of **1** with CO also led to reductive elimination of COE and to formation of the Ir(I) complex $[PhBP_3]Ir(CO)_2$.[6]

In the absence of trapping ligands, thermolysis of **3** in benzene-d_6 solvent (80 °C, 14 h) resulted in elimination of 1,3-COD, but no tractable Ir−H products were formed. No precipitate indicative of a dimeric polyhydride product[6] was observed. Attempts to prepare polyhydride complexes by reaction of **3** with H_2 (1 atm) in benzene-d_6 also did not lead to tractable Ir−H products, suggesting that in the absence of a strongly coordinating ligand, such as a phosphine or CO, the electronically and coordinatively unsaturated intermediate "$[PhBP_3']Ir(H)_2$" is highly reactive and does not form an isolable dimeric species. By comparison, the highly insoluble dihydride dimer $\{[PhBP_3]Ir(H)(\mu\text{-}H)\}_2$ formed readily, with concomitant elimination of COE, in the reaction of **1** with H_2.[6]

Scheme 3

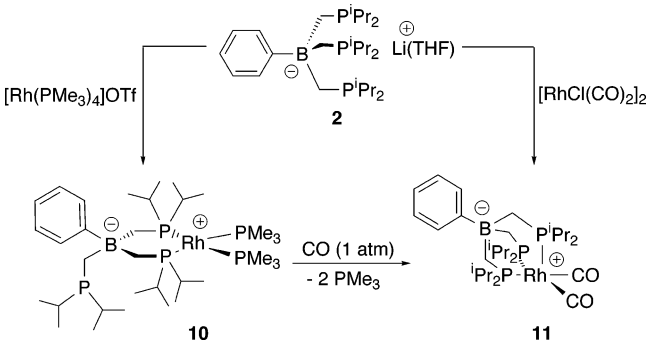

Synthesis and Characterization of [PhBP$_3$′]Rh(I) Complexes. The prominence of rhodium in E−H bond activation chemistry[2,12] prompted us to develop the synthesis of tris(phosphino)borate-chelated rhodium complexes. Accordingly, reactions of [PhBP$_3$′]Li(THF) with a number of Rh(I) starting materials were examined. It was found that [PhBP$_3$′]Li(THF) reacted over the course of a few minutes at room temperature with $(PMe_3)_4$RhOTf to generate LiOTf, 2 equiv of PMe_3, and the 16 e$^-$ Rh(I) complex [κ^2-PhB($CH_2P^iPr_2$)$_3$]Rh(PMe_3)$_2$ (**10**, Scheme 3), which forms quantitatively by ^{1}H and ^{31}P NMR spectroscopy (benzene-d_6). Compound **10** was isolated as an orange crystalline solid from pentane in 45% yield. The ^{31}P{^{1}H} NMR spectrum of **10** (benzene-d_6) exhibits three sets of resonances in the ratio 2:1:2; the two [PhBP$_3$′] phosphine donors chelating the rhodium center are observed as a complex multiplet at 49.42 ppm, while the resonance corresponding to the two PMe_3 ligands bound to rhodium is observed as a similar complex multiplet at −23.14 ppm. By comparison, the ^{31}P{^{1}H} NMR resonance corresponding to the free arm of [PhBP$_3$′] is observed as a singlet at 1.93 ppm.

Compound **10** reacted instantly with CO (1 atm) at room temperature in benzene-d_6 solution to generate 2 equiv of PMe_3 and [PhB($CH_2P^iPr_2$)$_3$]Rh(CO)$_2$ (**11**), indicating that the PMe_3 ligands of **10** are labile (Scheme 3). Compound **11** could also be prepared directly by the reaction of [PhBP$_3$′]Li(THF) with $[(CO)_2RhCl]_2$ (Scheme 3). Both reactions are quantitative by ^{1}H and ^{31}P NMR spectroscopy. By the latter route, **11** was isolated in 64% yield as a yellow crystalline solid. Unlike the bis-PMe_3 complex (**10**), all three phosphine donors of the [PhBP$_3$′] ligand appear equivalent on the NMR time scale at room temperature (benzene-d_6 solution), with the ^{31}P{^{1}H} NMR spectrum of **11** exhibiting only one resonance for the rhodium-bound phosphorus atoms at δ 37.51 ($^1J_{PRh}$ = 97 Hz). Variable-temperature ^{31}P NMR studies (toluene-d_8) indicate that this 3-fold symmetry is retained at temperatures down to −80 °C. At room temperature, the Rh-bound CO carbons are observed as a doublet of quartets in the ^{13}C{^{1}H} NMR spectrum of **11** (benzene-d_6), consistent with coupling to three equivalent phosphorus nuclei ($^2J_{CP}$ = 23 Hz) and to the Rh center ($^1J_{CRh}$ = 56 Hz).

The IR stretching frequencies of the metal-bound carbonyls for **11** and the analogous Tp^{Me2} and Cp* (Cp* = C_5Me_5) rhodium complexes (measured in hexanes) are shown in Table 3.[13,14] The trend displayed by these frequencies suggests that, to a general approximation, [PhBP$_3$′] is a more electron-donating ligand than both Tp^{Me2} and Cp*. A related cationic dicarbonyl complex, [(triphos)Rh(CO)$_2$][PF$_6$], has CO stretching frequencies of 2060 and 1995 cm^{-1} (measured in CH_2Cl_2),[15] indicating that the zwitterionic complex **11** is a significantly more electron-rich species.

Table 3. CO Stretching Frequencies for LRh(CO)$_2$ Complexes in Hexanes

complex	ν(CO), cm^{-1}
[PhBP$_3$′]Rh(CO)$_2$	2018, 1948
Cp*Rh(CO)$_2$	2026, 1964[a]
Tp^{Me2}Rh(CO)$_2$	2054, 1981[b]

[a] Ref 13. [b] Ref 14.

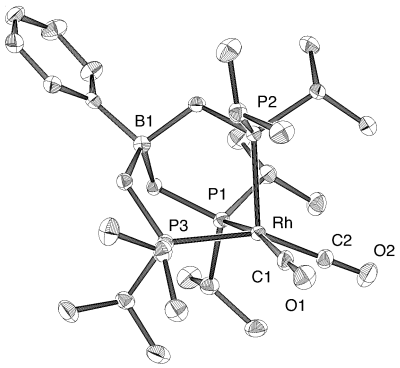

Figure 3. Crystallographically determined structure of [PhB($CH_2P^iPr_2$)$_3$]Rh(CO)$_2$ (**11**) depicted with 50% thermal ellipsoids; all hydrogen atoms have been omitted for clarity.

Table 4. Selected Bond Distances (Å) and Angles (deg) for 11

(a) Bond Distances			
Rh−P1	2.3771(8)	Rh−C1	1.889(3)
Rh−P2	2.4380(8)	Rh−C2	1.891(3)
Rh−P3	2.3876(8)		
(b) Bond Angles			
P1−Rh−P2	89.36(3)	C1−Rh−P2	103.48(10)
P1−Rh−P3	88.06(3)	C1−Rh−P3	90.27(9)
P2−Rh−P3	90.27(3)	C2−Rh−P1	89.95(10)
C1−Rh−C2	86.1(1)	C2−Rh−P2	115.05(9)
C1−Rh−P1	167.06(10)	C2−Rh−P3	154.58(10)

The solid state structure of complex **11** was determined by X-ray crystallography and is shown in Figure 3. Selected bond lengths and angles are summarized in Table 4. The metal center is five-coordinate, which is consistent with increased Lewis acidity at rhodium (relative to **10**) caused by the electron-withdrawing carbonyl ligands. The geometry at rhodium is that of a distorted square-based pyramid, with two arms of the [PhBP$_3$′] ligand and two CO ligands occupying the basal positions. Thus, P1 and C1 are *trans* to one another with a P1−Rh−C1 angle of 167.06(10)°, and P3 and C2 are also *trans* to each other with a somewhat compressed P3−Rh−C2 angle of 154.58(10)°. The phosphine donors *trans* to CO exhibit shorter Rh−P distances than the apical phosphine (Rh−P1 2.3771(8) Å, Rh−P3 2.3876(8) Å, Rh−P2 2.4380(8) Å).

(12) Jones, W. D.; Kakiuchi, F.; Murai, S. In *Topics in Organometallic Chemistry. Activation of Unreactive Bonds and Organic Synthesis*; Murai, S., Ed.; Springer: New York, 1999; Vol. 3, Chapters 2 and 3.

(13) Ghosh, C. K.; Graham, W. A. G. *J. Am. Chem. Soc.* **1987**, *109*, 4726.

(14) Johnston, G. G.; Baird, M. C. *Organometallics* **1989**, *8*, 1894.

(15) Ott, J.; Venanzi, L. M.; Ghilardi, C. A.; Midollini, S.; Orlandini, A. *J. Organomet. Chem.* **1985**, *291*, 89.

Scheme 4

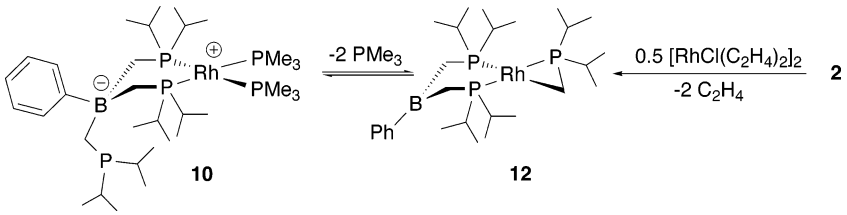

Complex **10** represents an interesting example of bidentate coordination for a tris(phosphino)borate ligand.[16] Numerous examples of analogous complexes featuring κ^2 coordination of Tp-derived ligands have been reported.[17] For example, a series of related Rh(I) bis(phosphine) complexes of the type Tp^{i}PrRhLL (LL = dppm, dppe, dppp; Tp^{i}Pr = hydridotri(3,5-diisopropylpyrazolyl)borate) were found to adopt square-planar geometries in the solid state, featuring κ^2-coordination of the Tp^{i}Pr ligand.[17e] In solution, studies have documented both κ^2 and κ^3 coordination for Tp^{R}Rh(LL) species, as well as cases of dynamic equilibria leading to κ^2−κ^3 isomerism.[17] The preference for bidentate or tridentate coordination was found to depend on several steric and electronic factors, including the nature of the substituents on the pyrazolyl rings, the nature of the donor ligands L, and the polarity of the solvent employed.[17c]

Although low-temperature NMR experiments did not provide evidence for κ^2 coordination of the [PhBP$_3$′] ligand for complex **11**, we pursued variable-temperature NMR studies of **10** in order to determine if in this instance κ^2−κ^3 interconversion is accessible on the NMR time scale. While the ^{31}P NMR spectrum of **10** is consistent with κ^2 coordination of the borate-derived ligand at room temperature (vide supra), a different species (**12**) was observed in toluene-d_8 solution at 80 °C. Inspection of the NMR features observed for **12** indicate that this species is not simply the κ^3-isomer of **10**.

The ^{31}P NMR spectrum of **12** (generated in situ from **10** at 80 °C in toluene-d_8) contains three multiplets at 76.99 (ddd, $^2J_{PPcis}$ = 24 Hz, $^2J_{PPcis}$ = 31 Hz, $^1J_{RhP}$ = 171 Hz), 70.31 (ddd, $^2J_{PPcis}$ = 24 Hz, $^2J_{PPtrans}$ = 241 Hz, $^1J_{RhP}$ = 187 Hz), and 13.92 (ddd, $^2J_{PPcis}$ = 31 Hz, $^2J_{PPtrans}$ = 241 Hz, $^1J_{RhP}$ = 108 Hz) ppm in a 1:1:1 ratio. The coupling constants measured for these three sets of resonances are consistent with two *cis*-P−P couplings, one *trans*-P−P coupling, and an additional coupling to Rh for each multiplet. Coupling between these three nuclei was further confirmed by ^{31}P,^{31}P-COSY NMR spectroscopy (toluene-d_8, 80 °C), which indicated off-diagonal cross-peaks correlating all three multiplets. Additionally, at 80 °C a broad resonance at −56 ppm suggested that exchange between coordinated and free PMe_3 occurs on the NMR time scale. A ^{31}P NMR spectrum identical to that observed for **10** was obtained upon cooling the solution back to room temperature, indicating that the formation of **12** is reversible. At intermediate temperatures, resonances corresponding to both **10** and **12** were observed by ^{31}P NMR spectroscopy with no indication of coalescence. Variable-temperature ^{1}H NMR studies of **10** (toluene-d_8) provided no evidence for the formation of rhodium hydrides in the 20−80 °C temperature range. In addition, similar ^{1}H and ^{31}P NMR spectroscopic features were observed in the 20−80 °C temperature range in methylcyclohexane-d_{14} solution, indicating that toluene activation is likely not playing a role in the formation of **12**.

To determine whether PMe_3 dissociation from **10** was indeed associated with the formation of **12**, 2 equiv of BPh_3 was added to a benzene-d_6 solution of **10**.[18] Precipitation of $Ph_3B(PMe_3)$ was observed within 10 min, and the room-temperature ^{31}P NMR spectrum of the reaction mixture indicated resonances identical to those observed for **12**. Subsequent addition of 2 equiv of PMe_3 to this reaction mixture gave rise to the original ^{31}P NMR spectrum observed for **10** at room temperature, confirming that **12** is indeed the product of PMe_3 dissociation from **10**. Furthermore, **12** could also be prepared independently in the absence of PMe_3 by the reaction of **2** with $[RhCl(C_2H_4)_2]_2$ (Scheme 4).

In an NMR-tube reaction, addition of 0.5 equiv of $[RhCl(C_2H_4)_2]_2$ to a benzene-d_6 solution of **2** resulted in an immediate color change from yellow to green-brown. The ^{31}P NMR spectrum of the reaction mixture indicated complete consumption of **2** and formation of a new Rh-containing product characterized by a ^{31}P NMR resonance at 59.40 ppm ($^2J_{RHP}$ = 126 Hz). The ^{1}H NMR spectrum of the reaction mixture did not exhibit resonances that could be assigned to the Rh-bound ethylene, although free ethylene was observed in solution. Over the course of 1 h at room temperature, the color of the reaction mixture changed from green-brown to orange. The ^{31}P NMR spectrum of the orange solution indicated disappearance of the resonance at 59.40 ppm and formation of a new Rh-containing species characterized by ^{31}P NMR features identical to those observed for **12**. This result confirms that the three phosphorus nuclei observed in the ^{31}P NMR spectrum of **12** are derived only from the [PhBP$_3$′] ligand.

On a preparative scale, a benzene solution of **2** and 0.5 equiv of $[RhCl(C_2H_4)_2]_2$ was allowed to stir at room temperature for 1 h, after which the volatile components of the reaction mixture were removed in vacuo. Crystallization from Et_2O afforded **12** as a red-orange crystal-

(16) Peters and co-workers have recently reported examples of transition metal complexes featuring bis(phosphino)borate ligands: (a) Thomas, J. C.; Peters, J. C. *J. Am. Chem. Soc.* **2001**, *123*, 5000. (b) Lu, C. C.; Peters, J. C. *J. Am. Chem. Soc.* **2002**, *124*, 5272. (c) Thomas, J. C.; Peters, J. C. *J. Am. Chem. Soc.* **2003**, *125*, 8870. (d) Thomas, J. C.; Peters, J. C. *Inorg. Chem.* **2003**, *42*, 5055. (e) Betley, T. A.; Peters, J. C. *Angew. Chem., Int. Ed.* **2003**, *42*, 2385.

(17) (a) Trofimenko, S. *Chem. Rev.* **1993**, *93*, 943. (b) Slugovc, C.; Padilla-Martinez, I.; Sirol, S.; Carmona, E. *Coord. Chem. Rev.* **2001**, *213*, 129. (c) Bucher, U. E.; Currao, A.; Nesper, R.; Rüegger, H.; Venanzi, L.; Younger, E. *Inorg. Chem.* **1995**, *34*, 66. (d) Oldham, W. J., Jr.; Heinekey, D. M. *Organometallics* **1997**, *16*, 467. (e) Ohta, K.; Hashimoto, M.; Takahashi, Y.; Hikichi, S.; Akita, M.; Moro-oka, Y. *Organometallics* **1999**, *18*, 3234. (f) Kläui, W.; Schramm, D.; Peters, W.; Rheinwald, G.; Lang, H. *Eur. J. Inorg. Chem.* **2001**, 1415. (g) Cîrcu, V.; Fernandes, M. A.; Carlton, L. *Inorg. Chem.* **2002**, *41*, 3859.

(18) Dioumaev, V. K.; Ploessl, K.; Carroll, P. J.; Berry, D. H. *Organometallics* **2000**, *19*, 3374.

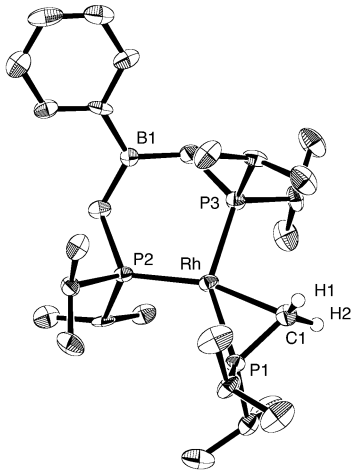

Figure 4. Crystallographically determined structure of $[PhB(CH_2P^iPr_2)_2]RhCH_2P^iPr_2$ (**12**) depicted with 50% thermal ellipsoids; all hydrogen atoms have been omitted for clarity, with the exception of H1 and H2.

line solid (87% yield) that exhibits ^{31}P NMR spectroscopic characteristics identical to those observed when the complex was generated in situ. The ^1H NMR spectrum of isolated **12** (benzene-d_6) shows no evidence for a rhodium hydride; however, an unusual doublet is observed at −0.11 ppm (J = 10 Hz). This resonance integrates as two hydrogens and is correlated to a ^{13}C NMR resonance at −19.9 ppm according to $^1H,^{13}C$-HMQC spectroscopy, suggesting the possibility of a Rh-bound methylene group. Further insight into the structure of **12** was provided by its ^{11}B NMR spectrum (benzene-d_6), which features a broad resonance at 74.9 ppm. The broad appearance of this resonance and its downfield shift correspond to a three-coordinate boron center, rather than the expected four-coordinate borate of the [PhBP$_3$′] ligand.[19] By comparison, the ^{11}B NMR resonance for **10** (benzene-d_6) is observed as a sharp singlet at −16.16 ppm. These results suggest that **12** is the product of an unusual migration of a ligand CH_2 group from boron to rhodium (Scheme 4).[20,21] Remarkably, this migration appears to be reversible in the presence of PMe_3, as observed in variable-temperature NMR experiments with **10** (Scheme 4). This was confirmed by addition of 2 equiv of PMe_3 to a benzene-d_6 solution of isolated **12**, which resulted in formation of **10**. Thus, it appears that under certain reaction conditions **12** functions effectively as a resting state for the "[PhBP$_3$′]Rh" fragment.

The structure of complex **12** was confirmed by X-ray crystallography and is shown in Figure 4. Selected bond lengths and angles are summarized in Table 5. The complex is monomeric in the solid state and features a three-membered Rh−P−C ring. The Rh center is four-coordinate and exhibits a distorted square planar geometry. Due to the constrained nature of the Rh−P1−C1 ring, the P1−Rh−C1 angle is compressed to 46.8(2)°. Accordingly, the remaining angles about the Rh center are larger than expected for an ideal square planar geometry (P1−Rh−P2 117.46(7)°, P2−Rh−P3 97.95(7)°, and C1−Rh−P3 97.7(2)°). The boron atom is three-coordinate and planar, with the sum of the three C−B−C angles summing to 359.8°. The Rh−B distance of 3.83 Å is well out of the range for a Rh−B interaction.[22]

Table 5. Selected Bond Distances(Å) and Angles (deg) for 12

(a) Bond Distances			
Rh−P1	2.239(2)	Rh−C1	2.187(8)
Rh−P2	2.240(2)	P1−C1	1.760(8)
Rh−P3	2.225(2)		
(b) Bond Angles			
P1−Rh−P2	117.46(7)	P2−Rh−P3	97.95(7)
P1−Rh−P3	144.56(8)	C1−Rh−P2	164.0(2)
P1−Rh−C1	46.8(2)	C1−Rh−P3	97.7(2)

The reaction of **2** with 0.5 equiv of $[(COE)_2RhCl]_2$ in benzene-d_6 solvent does not lead to formation of a Rh analogue of **3**. Rather, a mixture of **12** and additional unidentified Rh-containing products was observed by ^1H and ^{31}P NMR spectroscopy, with no indication for Rh−H formation.

Reactivity of [PhBP$_3$′]Rh(I) Complexes. Evidence for the facile dissociation of PMe_3 ligands from the coordinatively unsaturated Rh(I) center of complex **10** has been demonstrated by the ready conversion of **10** to the dicarbonyl complex, **11**, as well as by the observation of thermally induced ligand B−C bond activation leading to **12**. The lability of the PMe_3 ligands suggests that, under suitable conditions, **10** may undergo facile oxidative addition. However, reactions of **10** with polar substrates such as MeI or Me_3SiOTf in either benzene-d_6 or methylene chloride-d_2 solvents did not lead to formation of the oxidative addition products, possibly due to preferential reaction of these substrates with the free $-CH_2P^iPr_2$ arm of the [PhBP$_3$′] ligand.

By comparison, **10** reacted with H_2 (1 atm) at room temperature to yield the oxidative addition product $[PhBP_3']Rh(H)_2PMe_3$ (**13**) with loss of 1 equiv of PMe_3 (Scheme 5). Attempts to monitor this reaction by NMR spectroscopy (benzene-d_6) were hindered by the presence of 1 equiv of free PMe_3 in solution, which appears to exchange with coordinated PMe_3, leading to broad ^1H and ^{31}P NMR features. Compound **13** was isolated as an off-white solid in 76% yield, and as in the case of the Ir(III) complexes **7**, **8**, and **9**, it exhibits C_s symmetry in solution. The $^{31}P\{^1H\}$ NMR spectrum of **13** (benzene-d_6) contains three sets of resonances in a 1:2:1 ratio at 56.17 (ddt, [PhBP$_3$′] *trans* to PMe_3, $J_{PPtrans}$ = 332 Hz, J_{PPcis} = 25 Hz, J_{PRh} = 97 Hz), 32.00 (m, [PhBP$_3$′] *cis* to PMe_3), and −22.06 (ddt, *P*Me$_3$, $J_{PPtrans}$ = 330 Hz, J_{PPcis} = 24 Hz, J_{PRh} = 100 Hz) ppm, respectively. A Rh−H resonance integrating to two hydrogens is observed at −11.08 ppm by ^1H NMR spectroscopy (benzene-d_6).

(19) Kidd, R. G. *NMR of Newly Accessible Nuclei*; Academic Press: New York, 1983; Vol. 2.

(20) A related example involving alkylation of a nickel center by a tris((*tert*-butylthio)methyl)borate ligand has been reported: Schleber, P. J.; Mandimutsira, B. S.; Riordan, C. G.; Liable-Sands, L. M.; Incarvito, C. D.; Rheingold, A. L. *J. Am. Chem. Soc.* **2001**, *123*, 331. The alkylated nickel product retained an intact tris((*tert*-butylthio)-methyl)borate ligand set.

(21) Examples of intramolecular B−H bond activation in poly(pyrazolyl)borate metal chemistry have been reported: (a) Hill, A. F.; Owen, G. R.; White, A. J. P.; Williams, D. J. *Angew. Chem., Int. Ed.* **1999**, *38*, 2759. (b) Yeston, J. S.; Bergman, R. G. *Organometallics* **2000**, *19*, 2947, and references therein.

(22) The sum of the van der Waals radii for Rh and B is 3.5 Å. For comparison, the Rh−B distance for the Rh(I) σ-boryl complex $(PMe_3)_4$-Rh(B(cat)) (cat = 1,2-$O_2C_6H_4$) has been reported as 2.047(2) Å: Dai, C.; Stringer, G.; Marder, T. B.; Scott, A. J.; Clegg, W.; Norman, N. C. *Inorg. Chem.* **1997**, *36*, 272.

Scheme 5

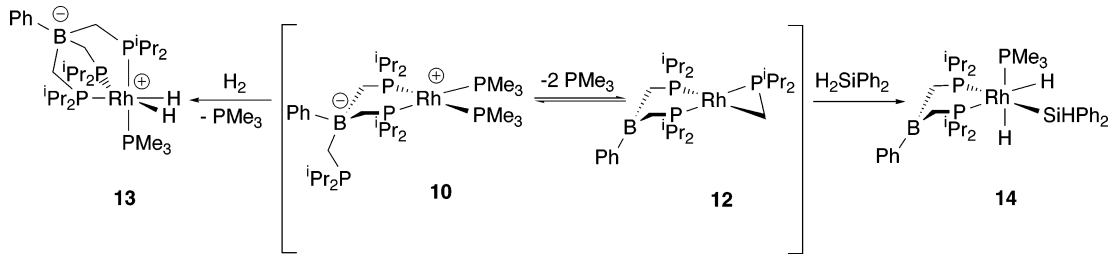

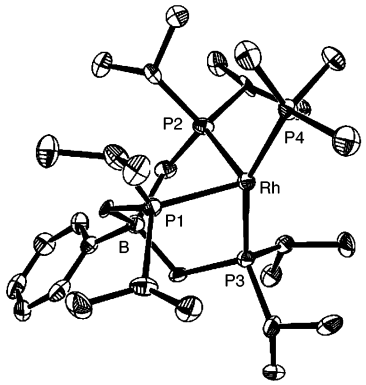

Figure 5. Crystallographically determined structure of $[PhB(CH_2P^iPr_2)_3]Rh(H)_2PMe_3$ (**13**) depicted with 50% thermal ellipsoids; all hydrogen atoms have been omitted for clarity.

Table 6. Selected Bond Distances (Å) and Angles (deg) for 13

	(a) Bond Distances		
Rh−P1	2.377(3)	Rh−P3	2.314(2)
Rh−P2	2.400(2)	Rh−P4	2.301(2)
	(b) Bond Angles		
P1−Rh−P2	89.15(8)	P2−Rh−P3	91.60(8)
P1−Rh−P3	90.13(9)	P2−Rh−P4	101.62(8)
P1−Rh−P4	109.46(9)	P3−Rh−P4	156.28(9)

The solid state structure of **13** was determined by X-ray crystallography and is shown in Figure 5. Selected bond lengths and angles are summarized in Table 6. The metrical parameters for **13** mirror those obtained for the Ir analogue, **7**. The tripodal phosphine ligand adopts the expected facial coordination featuring P−Rh−P angles of ca. 90°. As in the structure of **7**, the PMe_3 ligand is significantly tilted away from the two bulky isopropyl phosphine ligand arms (P4−Rh−P1 and P4−Rh−P2 angles of 109.46(9)° and 101.62(8)°, respectively), resulting in a P4−Rh−P3 angle of 156.28(9)°. Although the position of the hydride ligands was not determined, their approximate location is indicated by the open coordination sites *trans* to P1 and P2.

The reaction of **10** with secondary silanes (H_2SiR_2, with R = Et, Ph) in benzene-d_6 solvent at room temperature led to broad ^1H and ^{31}P NMR features, as previously observed in the reaction of **10** with H_2. A broad resonance was observed at −10.6 ppm in the ^1H NMR spectrum of the reaction mixture, consistent with the formation of a rhodium hydride species. On a preparative scale, the reaction of **10** with H_2SiPh_2 was allowed to stir at room temperature for 18 h, after which the volatile components of the reaction mixture were removed in vacuo. Upon crystallization from Et_2O, a yellow crystalline solid was isolated in <50% yield (**14**). The ^{31}P NMR spectrum of **14** (benzene-d_6) contains two

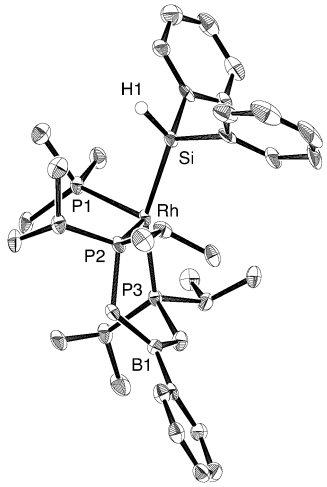

Figure 6. Crystallographically determined structure of $[PhB(CH_2P^iPr_2)_2]Rh(H)_2(SiHPh_2)(PMe_3)$ (**14**) depicted with 50% thermal ellipsoids; all hydrogen atoms have been omitted for clarity, with the exception of H1.

Table 7. Selected Bond Distances (Å) and Angles (deg) for 14

	(a) Bond Distances		
Rh−P1	2.355(2)	Rh−P3	2.341(2)
Rh−P2	2.353(2)	Rh−Si1	2.356(2)
	(b) Bond Angles		
P1−Rh−P2	110.41(5)	P2−Rh−P3	94.90(5)
P1−Rh−P3	104.52(5)	Si1−Rh−P3	155.27(6)

sets of resonances in a 2:1 ratio. Two overlapping multiplets integrating as two phosphorus nuclei are observed at 38.59 ppm, while a third multiplet integrating as one phosphorus is observed at −30.85 ppm ($^1J_{PRh}$ = 99 Hz). Characteristic features of the ^1H NMR spectrum of **14** include a broad Si−H resonance at 5.81 ppm ($^1J_{SiH}$ = 152 Hz), as well as two Rh−H resonances at −10.25 and −11.00 ppm integrating as one hydrogen each. The ^{11}B NMR spectrum of **14** contains a broad downfield-shifted resonance at 74.6 ppm, indicating that the ligand boron is three-coordinate.[19] These results are consistent with cleavage of a B−C bond in the ligand backbone and formation of a bis(phosphino)borane rhodium dihydride silyl complex that contains an additional phosphine donor (Scheme 5).

The structure of **14** was confirmed by X-ray crystallography and is shown in Figure 6. Selected bond lengths and angles are summarized in Table 7. A $-CH_2P^iPr_2$ ligand arm has been lost, and as a result, the boron atom is three-coordinate and planar, with the sum of the three C−B−C angles totaling 359.9°. The Rh−B distance is 3.94 Å, indicating that no bonding interaction exists between these two atoms. The Rh center is coordinated to the two phosphine arms of the

bis(phosphino)borane ligand, as well as to a diphenylsilyl group and a PMe_3 ligand. Although two rhodium hydride ligands are observed in solution by ^1H NMR spectroscopy, the positions of these two ligands were not determined in the solid state structure; their approximate location is indicated by the two empty coordination sites *trans* to P1 and P2.

The isolation of complex **14** from the reaction of **10** with H_2SiPh_2 indicates that under some reaction conditions the Rh-mediated B−C bond cleavage of the [$PhBP_3'$] ligand backbone may provide a facile decomposition pathway for [$PhBP_3'$]Rh complexes. Thus, while **10** appears stable indefinitely in benzene solution at room temperature, heating at 90 °C for 1 h resulted in decomposition to several unidentified Rh-containing species and the formation of MeP^iPr_2 (by ^1H and ^{31}P NMR spectroscopy).

The dicarbonyl complex **11** did not react appreciably with H_2 (1 atm, benzene-d_6) in the 20−70 °C temperature range or by photolysis (4 h). Heating of the reaction mixture at 90 °C over the course of 12 h resulted in decomposition to unidentified Rh-containing products. The ^1H NMR spectrum of the decomposition mixture featured a broad Rh−H resonance at −8.9 ppm. Evidence for the formation of MeP^iPr_2 was also observed under these conditions (by ^1H and ^{31}P NMR spectroscopy). The reaction of **11** with 1 equiv of H_2SiPh_2 (benzene-d_6) was similarly sluggish. Heating of the reaction mixture at 95 °C for 14 h resulted in a small amount of decomposition (<10%) of the dicarbonyl complex. Evidence was observed for the concomitant formation of both MeP^iPr_2 and $Ph_2HSiCH_2P^iPr_2$ (by ^1H and ^{31}P NMR spectroscopy). No evidence of a rhodium hydride complex was observed by ^1H NMR spectroscopy. Photolysis of the reaction mixture (6 h) also resulted in minor decomposition of **11** (<10%) and trace formation of MeP^iPr_2 and $Ph_2HSiCH_2P^iPr_2$ (by ^1H and ^{31}P NMR spectroscopy). Two rhodium hydride resonances were observed at −8.6 and −9.0 ppm in the ^1H NMR of this decomposition product mixture. In the absence of a secondary silane, photolysis of **11** in benzene-d_6 solvent for 4 h did not lead to any observed reaction.

Although the CO ligands of **11** proved difficult to displace thermally and photochemically, it was possible to chemically remove CO from **11** via reaction with Me_3NO. Thus, in the presence of 1 equiv of Me_3NO, **11** reacted with H_2 (1 atm) in benzene solvent at 65 °C to form the dihydride carbonyl complex **15**, with loss of Me_3N (eq 7). The formation of **15** was quantitative by

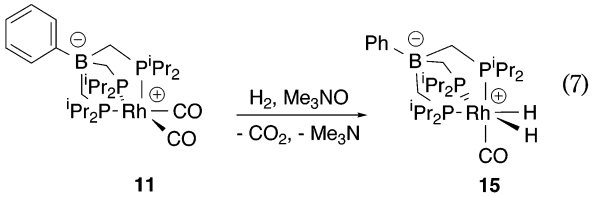

11 **15** (7)

^1H and ^{31}P NMR spectroscopy. Complex **15** exhibits spectroscopic features consistent with C_s symmetry in solution, as previously observed for the analogous Ir complex, **9**. A Rh−H resonance is observed by ^1H NMR spectroscopy at −8.99 ppm. In the absence of H_2, **11** did not react with Me_3NO in benzene solvent at 65 °C. At higher temperatures, decomposition to unidentified Rh-containing products was observed by ^1H and ^{31}P NMR spectroscopy.

The reaction of **11** with secondary silanes (H_2SiR_2, with R = Et, Ph) in the presence of 1 equiv of Me_3NO (benzene-d_6, 65 °C) leads to consumption of the silane (after 1 week for R = Ph, 12 h for R = Et) and ca. 60% conversion to the dihydride carbonyl complex **15**. This reaction appears to be complicated by the possibility of direct or Rh-mediated reactions of the silane with Me_3NO,[23] as evidence for numerous silicon-containing products is observed by ^{29}Si NMR analysis of the reaction mixture. The ^{29}Si NMR resonances observed fall in the 10 to −40 ppm region of the spectrum.

Concluding Remarks

This contribution describes the synthesis, characterization, and reactivity of zwitterionic rhodium and iridium complexes featuring the tris(phosphino)borate ligand $[PhB(CH_2P^iPr_2)_3]^-$ ([$PhBP_3'$]$^-$). The iridium allyl complex [$PhBP_3'$]IrH(η^3-C_8H_{13}) (**3**) provided a convenient entry to the chemistry of [$PhBP_3'$]Ir. Unlike its analogue [$PhBP_3$]IrH(η^3-C_8H_{13}) (**1**) ($PhBP_3$ = $PhB(CH_2PPh_2)_3$), which features P-phenyl substituents, **3** does not mediate "silylene extrusion" reactions; rather, the chemistry of **3** is dominated by facile β-hydride elimination of 1,3-cyclooctadiene. Thus, in reactions with secondary silanes, while **1** was found to reductively eliminate cyclooctene and give silylene dihydride complexes of the type [$PhBP_3$]Ir(H)$_2$(=SiR_2), reactions of compound **3** produced silyl-capped trihydride complexes of the type [$PhBP_3'$]Ir(H)$_3$($SiHR_2$) with concomitant elimination of 1,3-cyclooctadiene. While β-hydride elimination of 1,3-COD from **1** has been observed under certain reaction conditions, this complex serves as a source of "[$PhBP_3$]Ir" in its reactions with secondary silanes. By comparison, **3** has been found to react exclusively as a source of "[$PhBP_3'$]IrH_2". The observed preference for β-hydride elimination from **3** over reductive elimination may be attributed to the electron-rich nature of the iridium center, which should be less prone to undergo reduction processes.

The [$PhBP_3'$]IrH_2 fragment was readily trapped by the reaction of **3** with neutral donor ligands such as phosphines and CO. Interestingly, while previous results indicate that the [$PhBP_3$]IrH_2 fragment dimerizes to form the isolable complex {[$PhBP_3$]Ir(H)(μ-H)}$_2$, [$PhBP_3'$]IrH_2 does not appear to form an isolable dimer, suggesting that the P-isopropyl-substituted ligand is more sterically demanding than the P-phenyl analogue.

The [$PhBP_3'$] ligand also provided access to the first reported examples of tris(phosphino)borate-supported rhodium complexes. Although rhodium allyl complexes analogous to **3** do not appear to be accessible by comparable synthetic routes, the Rh(I) complexes [κ^2-$PhBP_3'$]Rh(PMe_3)$_2$ (**10**) and [$PhBP_3'$]Rh(CO)$_2$ were readily prepared and isolated. Complex **10** is an unusual example of κ^2-coordination of a tris(phosphino)borate ligand. By comparison, the dicarbonyl complex **11** is five-coordinate in the solid state.

(23) Hydrosilanes are known to reduce sulfoxides and phosphine oxides: (a) Fritzsche, H.; Hasserodt, U.; Korte, F. *Chem. Ber.* **1964**, *97*, 1988. (b) Naumann, K.; Zon, G.; Mislow, K. *J. Am. Chem. Soc.* **1969**, *91*, 2788. (c) Coumbe, T.; Lawrence, N. J.; Muhammad, F. *Tetrahedron Lett.* **1994**, *35*, 625. (d) Horner, L.; Balzer, W. D. *Tetrahedron Lett.* **1965**, 1157.

The CO ligands in complex **11** bind tightly to the electron-rich metal center and are not readily displaced thermally or photochemically. A comparison of the CO stretching frequencies of **11** with the related dicarbonyl complexes $Tp^{Me2}Rh(CO)_2$ and Cp*$Rh(CO)_2$ suggests that [$PhBP_3'$] is a stronger electron donor than both Tp^{Me2} and Cp*. By comparison, the PMe_3 ligands in complex **10** are labile in solution, and at temperatures above 20 °C evidence for an unusual dynamic process involving reversible dissociation of PMe_3 and migration of a ligand $-CH_2P^iPr_2$ group from B to Rh was observed. The product of this bond migration, [$PhB(CH_2P^iPr_2)_2$]-$RhCH_2P^iPr_2$ (**12**), can be isolated in high yield from the reaction of **2** with 0.5 equiv of $[RhCl(C_2H_4)_2]_2$. This ligand B−C bond activation appears to be a facile reaction pathway for [$PhBP_3'$]Rh complexes. Perhaps most surprising is the observation that this bond migration is reversible, depending on the reaction conditions employed, which suggests that **12** may be a viable masked source of "[$PhBP_3'$]Rh".

Experimental Section

General Procedures. All experiments were conducted under nitrogen in a Vacuum Atmospheres drybox or using standard Schlenk techniques. Dry, oxygen-free solvents were used unless otherwise indicated. Pentane was pretreated with concentrated H_2SO_4, 0.5 N $KMnO_4$ in 3 M H_2SO_4, and saturated $NaHCO_3$ solution, then dried over $MgSO_4$, stored over 4 Å molecular sieves, and distilled from potassium/benzophenone ketyl under a nitrogen atmosphere. Diethyl ether and THF were distilled under nitrogen from sodium/benzophenone ketyl. Toluene and benzene were pretreated with concentrated H_2SO_4, followed by saturated $NaHCO_3$ solution, and then dried over $MgSO_4$. Toluene was then distilled from molten sodium under a nitrogen atmosphere. Benzene was distilled from molten potassium under a nitrogen atmosphere. Benzene-d_6 and toluene-d_8 were degassed and stored over 4 Å molecular sieves. All NMR data were recorded at room temperature, unless otherwise noted, using either a Bruker AMX, AM, or DRX spectrometer. ^{1}H NMR spectra were referenced internally by the residual solvent proton signal relative to tetramethylsilane. ^{13}C NMR spectra were referenced internally by the ^{13}C signal of the NMR solvent relative to tetramethylsilane. ^{29}Si NMR spectra were referenced relative to an external standard of tetramethylsilane. ^{11}B NMR spectra were referenced using a $BF_3{\cdot}OEt_2$ external standard. ^{31}P NMR spectra were referenced relative to an 85% aqueous H_3PO_4 external standard. In some cases, distortionless enhancement by polarization transfer (DEPT) was used to assign the ^{13}C NMR resonances as CH_3, CH_2, CH, or C. Heteronuclear multiple quantum coherence (HMQC) was used to identify ^{1}H, ^{13}C coupling. Infrared spectra were recorded as Nujol mulls between NaCl plates using a Mattson FTIR spectrometer at a resolution of 4 cm^{-1}. Elemental analyses were performed by the College of Chemistry Microanalytical Laboratory at the University of California, Berkeley. Unless otherwise specified, all reagents were purchased from commercial suppliers and used without further purification. The compounds $[Ir(COE)_2Cl]_2$,[24] $(PMe_3)_4RhOTf$,[25] $[Rh(C_2H_4)_2Cl]_2$,[26] and $[Rh(CO)_2Cl]_2$[26] were prepared according to literature procedures.

[$PhB(CH_2P^iPr_2)_3$]Ir(H)(η^3-C_8H_{13}) (3). A benzene (5 mL) solution of [$PhB(CH_2P^iPr_2)_3$]Li(THF) (0.25 g, 0.45 mmol) was added to a stirred, room-temperature suspension of $[Ir(COE)_2Cl]_2$ (0.20 g, 0.22 mmol) in ca. 5 mL of benzene. The reaction mixture was allowed to stir at ambient temperature for 1 h. The volatile components of the reaction mixture were removed under vacuum, and the remaining yellow-orange residue was extracted into ca. 10 mL of benzene and filtered through Celite. The volatile material was removed under vacuum to afford **3** (0.32 g, 91%) as an analytically pure off-white solid. ^{1}H NMR (400 MHz, benzene-d_6): δ 7.97 (br m, 2 H, *o*-H_{arom}), 7.59 (t, 2 H, *m*-H_{arom}, $^3J_{HH}$ = 7 Hz), 7.34 (t, 1 H, *p*-H_{arom}, $^3J_{HH}$ = 7 Hz), 5.08 (m, 1 H, $CH_2CHCHCHCH_2$), 3.77 (m, 2 H, $CH_2CHCHCHCH_2$), 2.55 (br m, 4 H, CH_2), 2.20 (m, 2 H, $PCHMe_2$), 1.83 (m, 4 H, $PCHMe_2$), 1.58−1.44 (br m, 6 H, CH_2), 1.30−1.15 (m, 24 H, $PCHMe_2$), 0.98−0.90 (m, 16 H, $PCHMe_2$ + BCH_2P), 0.67 (br m, 2 H, BCH_2P), −15.30 (dt, 1 H, Ir*H*, $^2J_{HPtrans}$ = 120 Hz $^2J_{HPcis}$ = 17 Hz). ^{13}C{^{1}H} NMR (125.8 MHz, benzene-d_6): δ 132.1 (C_{arom}), 127.6 (C_{arom}), 123.8 (C_{arom}), 86.0 ($CH_2CHCHCHCH_2$), 48.6 ($CH_2CHCHCHCH_2$), 38.8 ($CH_2CHCHCHCH_2$), 35.6 (m, $PCHMe_2$), 34.2 (m, $PCHMe_2$), 30.8 ($CH_2CHCHCHCH_2$), 30.0 (m, $PCHMe_2$), 25.7 ($CH_2CHCHCHCH_2$), 20.7−18.7 ($PCHMe_2$), 15.2 (br, BCH_2P), 11.9 (br, BCH_2P). ^{31}P{^{1}H} NMR (162 MHz, benzene-d_6): δ 7.52 (d, 2 P, [$PhBP_3'$] *cis* to H, $^2J_{PP}$ = 21 Hz), −18.08 (t, 1 P, [$PhBP_3'$] *trans* to H, $^2J_{PP}$ = 21 Hz). ^{11}B NMR (160.46 MHz, benzene-d_6): δ −12.83. IR (cm^{-1}): 2152 m (IrH). Anal. Calcd for $C_{35}H_{67}BP_3Ir$: C, 53.63; H, 8.62. Found: C, 53.22; H, 8.89.

[$PhB(CH_2P^iPr_2)_3$]Ir(H)(η^3-C_3H_5) (4). A thick-walled, 500 mL flask fitted with a PTFE stopcock was charged with $[Ir(COE)_2Cl]_2$ (0.49 g, 0.55 mmol), a magnetic stirbar, and ca. 100 mL of THF. The slurry was cooled to −78 °C, and the headspace was evacuated. Propene (1 atm) was introduced and allowed to saturate the solution for ca. 2 min, at which point the flask was sealed and cooled with liquid nitrogen to give a frozen yellow solution. A solution of [$PhB(CH_2P^iPr_2)_3$]Li(THF) (0.50 g, 1.09 mmol) in 50 mL of THF was added to the frozen solution, which was then allowed to warm to ambient temperature and was stirred for 24 h. The volatile material was removed under vacuum, and the solid residue was extracted into ca. 10 mL of toluene. The toluene extracts were filtered through Celite and concentrated to ca. 3 mL. Storage of this solution at −35 °C for 24 h afforded **4** (0.52 g, 67%) as an off-white crystalline solid. ^{1}H NMR (500 MHz, benzene-d_6): δ 7.97 (br m, 2 H, *o*-H_{arom}), 7.58 (t, 2 H, *m*-H_{arom}, $^3J_{HH}$ = 8 Hz), 7.33 (t, 1 H, *p*-H_{arom}, $^3J_{HH}$ = 8 Hz), 4.51 (m, 1 H, CH_2CHCH_2), 2.72 (m, 2 H, CH_2), 2.65 (m, 2 H, CH_2), 2.15 (m, 2 H, $PCHMe_2$), 1.80 (m, 4 H, $PCHMe_2$), 1.32−1.09 (m, 24 H, $PCHMe_2$), 0.98 (m, 4 H, BCH_2P), 0.94−0.83 (m, 12 H, $PCHMe_2$), 0.70 (m, 2 H, BCH_2P), −15.60 (dt, 1 H, Ir*H*, $^2J_{PHtrans}$ = 130 Hz, $^2J_{PHcis}$ = 17 Hz). ^{13}C{^{1}H} NMR (125.8 MHz, benzene-d_6): δ 132.1 (C_{arom}), 123.9 (C_{arom}), 85.5 ($CH(CH_2)_2$), 36.3 (m, $PCHMe_2$), 34.4 (m, $PCHMe_2$), 30.3 (m, $PCHMe_2$), 26.5 ($CH(CH_2)_2$), 21.3 ($PCHMe_2$), 20.3 ($PCHMe_2$), 20.2 ($PCHMe_2$), 20.1 ($PCHMe_2$), 19.7 ($PCHMe_2$), 18.3 ($PCHMe_2$), 15.7 (br, BCH_2P), 11.5 (br, BCH_2P). ^{31}P{^{1}H} NMR (162 MHz, benzene-d_6): δ 9.53 (d, 2 P, [$PhBP_3'$] *cis* to H, $^2J_{PP}$ = 21 Hz), −20.15 (br m, 1 P, [$PhBP_3'$] *trans* to H). ^{11}B NMR (160.46 MHz, benzene-d_6): δ −12.31. IR (cm^{-1}): 2100 m (IrH). Anal. Calcd for $C_{30}H_{59}BP_3Ir$: C, 50.34; H, 8.31. Found: C, 50.52; H, 8.58.

[$PhB(CH_2P^iPr_2)_3$]IrH_3($SiHEt_2$) (5). Neat H_2SiEt_2 (0.023 g, 33 μL, 0.26 mmol) was added to a room-temperature benzene solution (ca. 10 mL) of **3** (0.20 g, 0.26 mmol). The reaction mixture was heated at 95 °C over the course of 14 h. The resulting orange solution was filtered through Celite, and the solvent was removed under vacuum to afford **5** as an off-white solid (0.19 g, 96%). ^{1}H NMR (400 MHz, benzene-d_6): δ 7.92 (br m, 2 H, *o*-H_{arom}), 7.59 (t, 2 H, *m*-H_{arom}, $^3J_{HH}$ = 8 Hz), 7.35 (t, 1 H, *p*-H_{arom}, $^3J_{HH}$ = 7 Hz), 5.78 (br s, 1 H, Si*H*Et_2, $^1J_{SiH}$ = 193 Hz), 1.74 (m, 6 H, $PCHMe_2$), 1.34−1.23 (m, 10 H, $SiEt_2$), 1.16 (m, 18 H, $PCHMe_2$), 1.05 (m, 18 H, $PCHMe_2$), 0.87 (br m, 6 H, BCH_2P), −12.27 (m, 3 H, Ir*H*). ^{13}C{^{1}H} NMR (100.6 MHz, benzene-d_6): δ 132.0 (C_{arom}), 127.7 (C_{arom}), 124.1 (C_{arom}), 32.3

(24) Herde, J. L.; Lambert, J. C.; Senoff, C. V. *Inorg. Synth.* **1974**, *15*, 18.
(25) (a) Thorn, D. L. *Organometallics* **1982**, *1*, 197. (b) Thorn, D. L. *Organometallics* **1985**, *4*, 192. (c) Aizenberg, M.; Milstein, D. *J. Chem. Soc., Chem. Commun.* **1994**, 411.
(26) Cramer, R. *Inorg. Synth.* **1974**, *15*, 14.

(m, P*C*HMe$_2$), 20.0 (PCH*Me*$_2$), 18.9 (PCH*Me*$_2$), 16.9 (Si*C*H$_2$-CH$_3$), 13.4 (br m, B*C*H$_2$P), 10.6 (SiCH$_2$*C*H$_3$). ^{31}P{^{1}H} NMR (162 MHz, benzene-d_6): δ 7.53 (s). ^{29}Si NMR (99.36 MHz, benzene-d_6): δ −19.8 (br q, $^2J_{SiP}$ = 5 Hz). ^{11}B NMR (160.46 MHz, benzene-d_6): δ −11.48. IR (cm^{-1}): 2070 (br, IrH), 2028 (SiH). Anal. Calcd for $C_{31}H_{67}BP_3SiIr$: C, 48.74; H, 8.84. Found: C, 48.73; H, 8.67.

[PhB(CH$_2$P^{i}Pr$_2$)$_3$]IrH$_3$(SiHPh$_2$) (6). Neat H_2SiPh_2 (0.047 g, 47 μL, 0.26 mmol) was added to a room-temperature benzene solution (ca. 10 mL) of **3** (0.20 g, 0.26 mmol). The reaction mixture was heated at 65 °C over the course of 14 h. The resulting orange solution was filtered through Celite, and the solvent was removed under vacuum to afford **6** as an off-white solid (0.20 g, 91%). ^{1}H NMR (400 MHz, benzene-d_6): δ 7.98 (d, 4 H, *o*-H$_{arom}$, $^3J_{HH}$ = 7 Hz), 7.90 (br d, 2 H, *o*-H$_{arom}$, $^3J_{HH}$ = 7 Hz), 7.57 (m, 2 H, *p*-H$_{arom}$, overlapping with 2 H, *m*-H$_{arom}$), 7.33 (t, 1 H, *p*-H$_{arom}$, $^3J_{HH}$ = 7 Hz), 7.25 (t, 4 H, *m*-H$_{arom}$, $^3J_{HH}$ = 7 Hz), 5.71 (s, 1 H, Si*H*Ph$_2$, $^1J_{SiH}$ = 193 Hz), 1.72 (m, 6 H, PC*H*Me$_2$), 0.99 (m, 36 H, PCH*Me*$_2$), 0.87 (br m, 6 H, BC*H*$_2$P), −11.55 (m, 3 H, Ir*H*). ^{13}C{^{1}H} NMR (100.6 MHz, benzene-d_6): δ 145.8 (C$_{arom}$), 136.2 (C$_{arom}$), 134.8 (C$_{arom}$), 131.9 (C$_{arom}$), 130.0 (C$_{arom}$), 127.4 (C$_{arom}$), 127.0 (C$_{arom}$), 32.2 (m, P*C*HMe$_2$), 19.7 (PCH*Me*$_2$), 19.0 (PCH*Me*$_2$), 12.8 (br, B*C*H$_2$P). ^{31}P{^{1}H} NMR (162 MHz, benzene-d_6): δ 7.85 (s). ^{29}Si NMR (99.36 MHz, benzene-d_6): δ −23.9 (br q, $^2J_{SiP}$ = 7 Hz). ^{11}B NMR (160.46 MHz, benzene-d_6): δ −11.54. IR (cm^{-1}): 2057 (br, IrH), 2025 (SiH). Anal. Calcd for $C_{39}H_{67}BP_3SiIr$: C, 54.47; H, 7.85. Found: C, 54.63; H, 7.94.

[PhB(CH$_2$P^{i}Pr$_2$)$_3$]Ir(H)$_2$(PMe$_3$) (7). Neat PMe$_3$ (26 μL, 0.019 g, 0.25 mmol) was added to a room-temperature benzene (5 mL) solution of **3** (0.20 g, 0.25 mmol). The resulting solution was heated at 60 °C for 24 h. The volatile material was removed under vacuum, and the remaining residue was extracted into ca. 3 mL of toluene. Storage of this solution at −35 °C over 24 h afforded **7** (0.13 g, 69%) as a white crystalline solid. ^{1}H NMR (500 MHz, benzene-d_6): δ 8.05 (br m, 2 H, *o*-H$_{arom}$), 7.61 (t, 2 H, *m*-H$_{arom}$, $^3J_{HH}$ = 8 Hz), 7.35 (tt, 1 H, *p*-H$_{arom}$, $^3J_{HH}$ = 7 Hz, $^4J_{HH}$ = 2 Hz), 2.04 (m, 2 H, PC*H*Me$_2$), 1.84 (m, 2 H, PC*H*Me$_2$), 1.66 (m, 2 H, PC*H*Me$_2$), 1.49 (dd, 9 H, P*Me*$_3$, $^2J_{HP}$ = 8 Hz, $^4J_{HPtrans}$ = 2 Hz), 1.38 (dd, 6 H, PCH*Me*$_2$, $^3J_{HH}$ = 14 Hz, $^3J_{HP}$ = 7 Hz), 1.31 (dd, 6 H, PCH*Me*$_2$, $^3J_{HH}$ = 13 Hz, $^3J_{HP}$ = 7 Hz), 1.23 (dd, 6 H, PCH*Me*$_2$, $^3J_{HH}$ = 17 Hz, $^3J_{HP}$ = 9 Hz), 1.20−1.15 (m, 12 H, PCH*Me*$_2$), 1.09 (br m, 4 H, BC*H*$_2$P), 0.98 (dd, 6 H, PCH*Me*$_2$, $^3J_{HH}$ = 13 Hz, $^3J_{HP}$ = 8 Hz), 0.87 (br m, 2 H, BC*H*$_2$P), −13.50 (m, 2 H, Ir*H*). ^{13}C{^{1}H} NMR (125.8 MHz, benzene-d_6): δ 132.3 (C$_{arom}$), 127.6 (C$_{arom}$), 123.7 (C$_{arom}$), 34.4 (m, P*C*HMe$_2$), 32.1 (m, P*C*HMe$_2$), 31.0 (m, P*C*HMe$_2$), 27.9 (m, P*Me*$_3$), 21.3 (PCH*Me*$_2$), 20.8 (PCH*Me*$_2$), 20.7 (PCH*Me*$_2$), 20.2 (PCH*Me*$_2$), 18.8 (PCH*Me*$_2$), 18.5 (PCH*Me*$_2$), 14.6 (br, B*C*H$_2$P). ^{31}P{^{1}H} NMR (162 MHz, benzene-d_6): δ 15.39 (dt, 1 P, [PhBP$_3$′] *trans* to PMe$_3$, $^2J_{PPtrans}$ = 286 Hz, $^2J_{PPcis}$ = 21 Hz), −2.15 (m, 2 P, [PhBP$_3$′] *cis* to PMe$_3$), −68.15 (dt, 1 P, Ir*P*Me$_3$, $^2J_{PPtrans}$ = 287 Hz, $^2J_{ppcis}$ = 21 Hz). ^{11}B NMR (160.46 MHz, benzene-d_6): δ −12.21. IR (cm^{-1}): 2106 (IrH), 2049 (IrH). Anal. Calcd for $C_{30}H_{64}BP_4Ir\cdot(C_7H_8)_{0.5}$: C, 50.43; H, 8.59. Found: C, 50.51; H, 8.58.

[PhB(CH$_2$P^{i}Pr$_2$)$_3$]Ir(H)$_2$PH$_2$Cy (8). Neat PH$_2$Cy (0.030 g, 34 μL, 0.26 mmol) was added to a room-temperature benzene solution (ca. 5 mL) of **3** (0.20 g, 0.26 mmol). The resulting orange solution was heated at 65 °C over the course of 14 h. The reaction mixture was filtered through Celite, and the solvent was removed under vacuum to afford **8** as an off-white solid (0.19 g, 92% yield). ^{1}H NMR (500 MHz, benzene-d_6): δ 8.02 (br d, 2 H, *o*-H$_{arom}$, $^3J_{HH}$ = 6 Hz), 7.61 (t, 2 H, *m*-H$_{arom}$, $^3J_{HH}$ = 7 Hz), 7.35 (t, 1 H, *p*-H$_{arom}$, $^3J_{HH}$ = 8 Hz), 4.38 (br d, 2 H, P*H*$_2$Cy, $^1J_{HP}$ = 316 Hz), 2.18 (br m, 2 H, P*Cy*), 2.06 (m, 2 H, PC*H*Me$_2$), 1.83 (m, 2 H, PC*H*Me$_2$), 1.66 (m, 5 H, PC*H*Me$_2$ + P*Cy*), 1.46 (br m, 2 H, P*Cy*), 1.40 (dd, 6 H, PCH*Me*$_2$, $^3J_{HH}$ = 15 Hz, $^3J_{HP}$ = 7 Hz), 1.33 (dd, 6 H, PCH*Me*$_2$, $^3J_{HH}$ = 14 Hz, $^3J_{HP}$ = 8 Hz), 1.22−1.10 (m, 26 H, PCH*Me*$_2$ + P*Cy* + BC*H*$_2$P), 0.96 (dd, 6 H, PCH*Me*$_2$, $^3J_{HH}$ = 13 Hz, $^3J_{HP}$ = 8 Hz), 0.86 (br m, 2 H, BC*H*$_2$P), −13.25 (m, 2 H, Ir−H). ^{13}C{^{1}H} NMR (125.8 MHz): δ 132.2 (C$_{arom}$), 127.6 (C$_{arom}$), 123.8 (C$_{arom}$), 38.5 (m, P*Cy*), 34.5 (m, P*C*HMe$_2$), 33.6 (P*Cy*), 32.0 (m, P*C*HMe$_2$), 31.6 (m, P*C*HMe$_2$), 27.2 (P*Cy*), 26.4 (P*Cy*), 21.4 (PCH*Me*$_2$), 20.7 (PCH*Me*$_2$), 19.6 (PCH*Me*$_2$), 18.8 (PCH*Me*$_2$), 18.7 (PCH*Me*$_2$), 14.7 (br, B*C*H$_2$P). ^{31}P{^{1}H} NMR (202 MHz, benzene-d_6): δ 16.36 (dt, 1 P, [PhBP$_3$′] *trans* to PH$_2$Cy, $^2J_{PPtrans}$ = 283 Hz, $^2J_{PPcis}$ = 20 Hz), −3.24 (m, 2 P, [PhBP$_3$′] *cis* to PH$_2$Cy), −64.06 (br d, 1 P, Ir*P*H$_2$Cy, $^2J_{PPtrans}$ = 287 Hz). ^{11}B NMR (160.46 MHz, benzene-d_6): δ −11.61. IR (cm^{-1}): 2313 (PH), 2292 (PH), 2046 (IrH). Anal. Calcd for $C_{33}H_{68}BP_4Ir$: C, 50.06; H, 8.66. Found: C, 49.96; H, 8.76.

[PhB(CH$_2$P^{i}Pr$_2$)$_3$]Ir(H)$_2$(CO) (9). A benzene solution (ca. 5 mL) of **3** (0.20 g, 0.26 mmol) was degassed via three freeze−pump−thaw cycles, and CO (1 atm) was introduced. The resulting orange solution was heated at 65 °C over the course of 14 h. The reaction mixture was filtered through Celite, and the solvent was removed under vacuum to afford **9** as a yellow solid (0.18 g, 97% yield). ^{1}H NMR (400 MHz, benzene-d_6): δ 7.89 (br m, 2 H, *o*-H$_{arom}$), 7.58 (t, 2 H, *m*-H$_{arom}$, $^3J_{HH}$ = 8 Hz), 7.34 (m, 1 H, *p*-H$_{arom}$), 2.00 (m, 2 H, PC*H*Me$_2$), 1.69 (m, 2 H, PC*H*Me$_2$), 1.60 (m, 2 H, PC*H*Me$_2$), 1.29−1.01 (m, 36 H, PCH*Me*$_2$), 0.87 (br m, 6 H, BC*H*$_2$P), −11.84 (m, 2 H, Ir−*H*). ^{13}C{^{1}H} NMR (100.6 MHz): δ 178.4 (dt, Ir*C*O, $^2J_{CPtrans}$ = 97 Hz, $^2J_{CPcis}$ = 5 Hz), 131.9 (C$_{arom}$), 127.7 (C$_{arom}$), 124.2 (C$_{arom}$), 33.5 (m, P*C*HMe$_2$), 33.2 (m, P*C*HMe$_2$), 31.0 (m, P*C*HMe$_2$), 20.8 (PCH*Me*$_2$), 20.2 (PCH*Me*$_2$), 20.0 (PCH*Me*$_2$), 19.2 (PCH*Me*$_2$), 18.6 (PCH*Me*$_2$), 18.4 (PCH*Me*$_2$), 13.17 (br, B*C*H$_2$P). ^{31}P{^{1}H} NMR (162 MHz, benzene-d_6): δ 11.47 (t, 1 P, [PhBP$_3$′] *trans* to CO, $^2J_{PPcis}$ = 24 Hz), 3.75 (d, 2 P, [PhBP$_3$′] *cis* to CO, $^2J_{PP}$ = 24 Hz). ^{11}B NMR (160.46 MHz, benzene-d_6): δ −11.23. IR (cm^{-1}): 2003 (CO), 1939 (IrH), 1926 (IrH). Anal. Calcd for $C_{28}H_{55}BP_3OIr$: C, 47.79; H, 7.88. Found: C, 48.18; H, 7.78.

[κ^2-PhB(CH$_2$P^{i}Pr$_2$)$_3$]Rh(PMe$_3$)$_2$ (10). A benzene (5 mL) solution of [PhB(CH$_2$P^{i}Pr$_2$)$_3$]Li(THF) (0.20 g, 0.36 mmol) was added to a stirred, room-temperature suspension of Rh(PMe$_3$)$_4$-OTf (0.20 g, 0.36 mmol) in ca. 5 mL of benzene. The resulting orange solution was allowed to stir at room temperature for 1 h. The volatiles were removed under vacuum, and the remaining orange residue was extracted into ca. 20 mL of pentane. The pentane extracts were filtered through Celite, and the volume was reduced by 50% under vacuum. Storage of this solution at −35 °C for 24 h afforded **10** (0.12 g, 45%) as orange microcrystals. ^{1}H NMR (500 MHz, benzene-d_6): δ 8.05 (br m, 2 H, *o*-H$_{arom}$), 7.50 (t, 2 H, *m*-H$_{arom}$, $^3J_{HH}$ = 8 Hz), 7.28 (m, 1 H, *p*-H$_{arom}$), 1.89 (m, 2 H, PC*H*Me$_2$), 1.75 (m, 2 H, PC*H*Me$_2$), 1.54 (m, 2 H, PC*H*Me$_2$), 1.45−0.94 (m, 36 H, PCH*Me*$_2$), 0.86 (br d, 20 H, RhP*Me*$_3$ + BC*H*$_2$P, J_{HP} = 8 Hz), 0.68 (br m, 4 H, BC*H*$_2$P). ^{13}C{^{1}H} NMR (125.8 MHz, benzene-d_6): δ 133.6 (C$_{arom}$), 126.5 (C$_{arom}$), 123.2 (C$_{arom}$), 30.3 (m, P*C*HMe$_2$), 29.5 (m, P*C*HMe$_2$), 24.5 (m, P*C*HMe$_2$), 21.8−19.9 (PCH*Me*$_2$ + P*Me*$_3$), 16.0 (br, BC*H*$_2$P), 13.39 (br, BC*H*$_2$P). ^{31}P{^{1}H} NMR (162 MHz, benzene-d_6): δ 49.42 (m, 2 P, ^{i}Pr$_2$*P*Rh), 1.93 (s, 1 P, BCH$_2$*P*^{i}Pr$_2$), −23.14 (m, 2 P, Rh*P*Me$_3$). ^{11}B NMR (160.46 MHz, benzene-d_6): δ −16.16. Anal. Calcd for $C_{33}H_{71}BP_5Rh$: C, 53.82; H, 9.72. Found: C, 53.87; H, 9.89.

[PhB(CH$_2$P^{i}Pr$_2$)$_3$]Rh(CO)$_2$ (11). Solid [RhCl(CO)$_2$]$_2$ (0.070 g, 0.18 mmol) was added to a room-temperature benzene solution (ca. 15 mL) of [PhB(CH$_2$P^{i}Pr$_2$)$_3$]Li(THF) (0.20 g, 0.36 mmol). The resulting orange solution was allowed to stir at room temperature for 2 h. The solvent was removed under vacuum, and the residue was extracted into ca. 30 mL of Et$_2$O. The Et$_2$O extracts were filtered through Celite and concentrated to ca. 5 mL volume. The solution was then refrigerated at −30 °C overnight to afford **11** (0.15 g, 64%) as a yellow crystalline solid. Alternatively **11** can be prepared by treating **10** with 1 atm of CO at room temperature in benzene solution. ^{1}H NMR (400 MHz, benzene-d_6): δ 7.87 (br m, 2 H, *o*-H$_{arom}$), 7.56 (t, 2 H, *m*-H$_{arom}$, $^3J_{HH}$ = 8 Hz), 7.32 (t, 1 H, *p*-H$_{arom}$, $^3J_{HH}$ = 7 Hz), 1.75 (m, 6 H, PC*H*Me$_2$), 1.22 (m, 18 H, PCH*Me*$_2$), 1.07 (m, 18 H, PCH*Me*$_2$), 0.80 (br m, 6 H, BC*H*$_2$P). ^{13}C NMR

(100.6 MHz, benzene-d_6): δ 204.4 (dq, Rh*C*O, $^1J_{CRh}$ = 56 Hz, $^2J_{CP}$ = 23 Hz), 131.8 (C_{arom}), 127.7 (C_{arom}), 124.1 (C_{arom}), 32.8 (m, P*C*HMe$_2$), 20.7 (PCH*Me*$_2$), 19.1 (PCH*Me*$_2$), 14.8 (br, B*C*H$_2$P). ^{31}P{^{1}H} NMR (162 MHz, benzene-d_6): δ 37.51 (d, $^1J_{RhP}$ = 97 Hz). ^{11}B NMR (160.46 MHz, benzene-d_6): δ −13.89. IR (cm^{-1}): 2007 (CO), 1935 (CO). Anal. Calcd for $C_{29}H_{53}BP_3O_2Rh$: C, 54.39; H, 8.34. Found: C, 54.55; H, 8.29.

[PhB(CH$_2$P^{i}Pr$_2$)$_2$]RhCH$_2$P^{i}Pr$_2$ (12). Solid [RhCl(C$_2$H$_4$)$_2$]$_2$ (0.070 g, 0.18 mmol) was added to a room-temperature benzene solution (ca. 15 mL) of [PhB(CH$_2$P^{i}Pr$_2$)$_3$]Li(THF) (0.20 g, 0.36 mmol). The resulting green-brown solution was allowed to stir at room temperature for 1 h. The solvent was removed under vacuum, and the remaining residue was extracted into ca. 15 mL of Et$_2$O. The Et$_2$O extract was filtered through Celite, concentrated to ca. 3 mL volume, and refrigerated at −30 °C overnight to give **12** as a red crystalline solid (0.18 g, 87% yield). ^{1}H NMR (500 MHz, benzene-d_6): δ 8.04 (m, 2 H, *o*-H$_{arom}$), 7.30 (m, 3 H, *m*-H$_{arom}$ + *p*-H$_{arom}$), 2.22 (m, 2 H, PC*H*Me$_2$), 2.14 (m, 2 H, PC*H*Me$_2$), 1.88 (m, 2 H, PC*H*Me$_2$), 1.68 (m, 4 H, BC*H*$_2$P), 1.26 (m, 12 H, PCH*Me*$_2$), 1.17−1.03 (m, 24 H, PCH*Me*$_2$), −0.11 (d, 2 H, *J* = 10 Hz). ^{13}C{^{1}H} NMR (125.8 MHz, benzene-d_6): δ 142.2 (C_{arom}), 134.9 (C_{arom}), 132.6 (C_{arom}), 128.2 (C_{arom}), 30.6 (m, P*C*HMe$_2$), 30.1 (m, P*C*HMe$_2$), 23.2 (br, B*C*H$_2$P), 21.9 (br, B*C*H$_2$P), 21.6 (m, P*C*HMe$_2$), 20.6 (PCH*Me*$_2$), 20.2 (PCH*Me*$_2$), 20.1 (PCH*Me*$_2$), 20.0 (PCH*Me*$_2$), 19.9 (PCH*Me*$_2$), 19.2 (PCH*Me*$_2$), 19.1 (PCH*Me*$_2$), −19.9 (m, Rh*C*H$_2$). ^{31}P{^{1}H} NMR (202 MHz, benzene-d_6): δ 76.99 (ddd, 1 P, $^2J_{PPcis}$ = 24 Hz, $^2J_{PPcis}$ = 31 Hz, $^1J_{RhP}$ = 171 Hz), 70.31 (ddd, 1 P, $^2J_{PPcis}$ = 24 Hz, $^2J_{PPtrans}$ = 241 Hz, $^1J_{RhP}$ = 187 Hz), 13.92 (ddd, 1 P, $^2J_{PPcis}$ = 31 Hz, $^2J_{PPtrans}$ = 241 Hz, $^1J_{RhP}$ = 108 Hz). ^{11}B NMR (160.46 MHz, benzene-d_6): δ 74.9 (br). Anal. Calcd for $C_{27}H_{53}BP_3Rh$: C, 55.50; H, 9.14. Found: C, 55.70; H, 9.44.

[PhB(CH$_2$P^{i}Pr$_2$)$_3$]Rh(H)$_2$PMe$_3$ (13). A thick-walled, 100 mL flask fitted with a PTFE stopcock was charged with **10** (0.66 g, 0.90 mmol), a magnetic stirbar, and ca. 10 mL of benzene. The resulting orange solution was degassed via three freeze−pump−thaw cycles, and hydrogen (1 atm) was introduced. The flask was sealed off, and the resulting pale yellow reaction mixture was allowed to stir at ambient temperature for 24 h. The volatile material was removed under vacuum, and the remaining pale yellow residue was washed with 3 × 5 mL of pentane and dried under vacuum to give **13** (0.45 g, 76%) as an analytically and spectroscopically pure pale yellow solid. ^{1}H NMR (500 MHz, benzene-d_6): δ 8.04 (br m, 2 H, *o*-H$_{arom}$), 7.60 (t, 2 H, *m*-H$_{arom}$, $^3J_{HH}$ = 7 Hz), 7.33 (t, 1 H, *p*-H$_{arom}$, $^3J_{HH}$ = 7 Hz), 1.92 (m, 2 H, PC*H*Me$_2$), 1.72 (m, 2 H, PC*H*Me$_2$), 1.61 (m, 2 H, PC*H*Me$_2$), 1.38 (dd, 6 H, PCH*Me*$_2$, $^3J_{HH}$ = 7 Hz, $^3J_{PH}$ = 15 Hz), 1.30 (m, 12 H, PCH*Me*$_2$), 1.19 (m, 21 H, PCH*Me*$_2$ + P*Me*$_3$) 1.01 (dd, 6 H, PCH*Me*$_2$, $^3J_{HH}$ = 7 Hz, $^3J_{HP}$ = 12 Hz), 0.94 (br m, 4 H, BC*H*$_2$P), 0.78 (br m, 2 H, BC*H*$_2$P), −11.08 (m, 2 H, Rh*H*). ^{13}C{^{1}H} NMR (125.8 MHz, benzene-d_6): δ 132.1 (C_{arom}), 127.5 (C_{arom}), 123.6 (C_{arom}), 34.1 (m, P*C*HMe$_2$), 31.1 (m, P*C*HMe$_2$), 30.7 (m, P*C*HMe$_2$), 27.2 (m, P*Me*$_3$), 21.3 (PCH*Me*$_2$), 20.9 (PCH*Me*$_2$), 19.9 (PCH*Me*$_2$), 19.1 (PCH*Me*$_2$), 16.2 (br, B*C*H$_2$P), 14.87 (br, B*C*H$_2$P). ^{31}P{^{1}H} NMR (162 MHz, benzene-d_6): δ 56.17 (ddt, 1 P, [PhBP$_3$′] *trans* to PMe$_3$, $^2J_{PPtrans}$ = 332 Hz, $^1J_{PRh}$ = 97 Hz, $^2J_{PPcis}$ = 25 Hz), 32.00 (m, 2 P, [PhBP$_3$′] cis to PMe$_3$), −22.06 (ddt, 1 P, *P*Me$_3$, $^2J_{PPtrans}$ = 330 Hz, $^1J_{PRh}$ = 100 Hz, $^2J_{PPcis}$ = 24 Hz). ^{11}B NMR (160.46 MHz, benzene-d_6): δ −13.82. IR (cm^{-1}): 2011 (RhH), 1945 (RhH). Anal. Calcd for $C_{30}H_{64}BP_4Rh$: C, 54.39; H, 9.74. Found: C, 54.51; H, 9.83.

[PhB(CH$_2$P^{i}Pr$_2$)$_2$]Rh(H)$_2$(SiHPh$_2$)(PMe$_3$) (14). Neat Ph$_2$SiH$_2$ (0.05 mL, 0.27 mmol) was added to a room-temperature benzene (ca. 10 mL) solution of **10** (0.20 g, 0.27 mmol). The reaction mixture was allowed to stand at room temperature over the course of 18 h. The solution was filtered through Celite, and the solvent was removed under vacuum. The remaining residue was dissolved in ca. 3 mL of Et$_2$O and refrigerated at −30 °C overnight to give **14** as a pale yellow crystalline solid (0.084 g, 44%). ^{1}H NMR (500 MHz, benzene-d_6): δ 8.26 (br m, 4 H, *o*-H$_{arom}$), 7.70 (d, 2 H, *o*-H$_{arom}$, J_{HH} = 7 Hz), 7.34 (m, 7 H, H$_{arom}$), 7.04 (m, 2 H, H$_{arom}$), 5.81 (br s, 1 H, Si*H*, $^1J_{HSi}$ = 152 Hz), 1.95−1.60 (br m, 4 H, PC*H*Me$_2$), 1.27−0.81 (br m, 37 H, PCH*Me*$_2$ + P*Me*$_3$ + BC*H*$_2$P), −10.25 (m, 1 H, Rh−*H*), −11.00 (m, 1 H, Rh−*H*). ^{13}C{^{1}H} NMR (125.8 MHz, benzene-d_6): δ 136.2 (C_{arom}), 136.0 (C_{arom}), 133.8 (C_{arom}), 132.3 (C_{arom}), 127.4 (C_{arom}), 127.1 (C_{arom}), 126.6 (C_{arom}), 31.0 (m, P*C*HMe$_2$), 28.4 (m, P*C*HMe$_2$), 28.1 (m, P*C*HMe$_2$), 26.9 (m, P*C*HMe$_2$), 24.0 (m, P*Me*$_3$), 23.1−18.4 (PCH*Me*$_2$), 18.0 (br, B*C*H$_2$P), 15.6 (br, B*C*H$_2$P). ^{31}P{^{1}H} NMR (202 MHz, benzene-d_6): δ 38.59 (m, 2 P, BCH$_2$*P*^{i}Pr$_2$), −30.85 (m, 1 P, Rh*P*Me$_3$). ^{29}Si NMR (99.36 MHz, benzene-d_6): δ 19.6 (br d, $^1J_{SiRh}$ = 239 Hz). ^{11}B NMR (160.46 MHz, benzene-d_6): δ 74.6. IR (cm^{-1}): 2008, 1982, 1947. Anal. Calcd for $C_{35}H_{59}BP_3SiRh$: C, 58.83; H, 8.32. Found: C, 58.59; H, 8.08.

[PhB(CH$_2$P^{i}Pr$_2$)$_3$]Rh(H)$_2$CO (15). A thick-walled, 100 mL flask fitted with a PTFE stopcock was charged with **8** (0.12 g, 0.19 mmol), Me$_3$NO (0.014 g, 0.19 mmol), a magnetic stirbar, and ca. 10 mL of benzene. The resulting orange solution was degassed via three freeze−pump−thaw cycles, and hydrogen (1 atm) was introduced. The flask was sealed off, and the reaction mixture was allowed to stir at 70 °C for 14 h. The volatiles were removed under vacuum, and the remaining yellow residue was extracted into Et$_2$O (ca. 10 mL). The Et$_2$O extracts were filtered through Celite, concentrated to ca. 3 mL, and refrigerated at −30 °C overnight to give off-white crystals of **15** (0.10 g, 86%). ^{1}H NMR (500 MHz, benzene-d_6): δ 7.89 (d, 2 H, *o*-H$_{arom}$, $^3J_{HH}$ = 6 Hz), 7.57 (t, 2 H, *m*-H$_{arom}$, $^3J_{HH}$ = 7 Hz), 7.33 (t, 1 H, *p*-H$_{arom}$, $^3J_{HH}$ = 7 Hz), 1.86 (m, 2 H, PC*H*Me$_2$), 1.56 (m, 4 H, PC*H*Me$_2$), 1.28 (dd, 6 H, PCH*Me*$_2$, $^3J_{HH}$ = 7 Hz, $^3J_{HP}$ = 15 Hz), 1.22 (dd, 6 H, PCH*Me*$_2$, $^3J_{HH}$ = 7 Hz, $^3J_{HP}$ = 15 Hz), 1.16 (dd, 6 H, PCH*Me*$_2$, $^3J_{HH}$ = 7 Hz, $^3J_{HP}$ = 15 Hz), 1.11−1.03 (m, 18 H, PCH*Me*$_2$), 0.88 (br m, 2 H, BC*H*$_2$P), 0.77 (br m, 4 H, BC*H*$_2$P), −8.99 (m, 2 H, Rh*H*). ^{13}C{^{1}H} NMR (100.6 MHz, benzene-d_6): δ 197.4 (ddt, Rh*C*O, $^2J_{CPtrans}$ = 107 Hz, $^1J_{CRh}$ = 52 Hz, $^2J_{CPcis}$ = 7 Hz), 131.8 (*o*-C$_{arom}$), 127.1 (*m*-C$_{arom}$), 124.1 (*p*-C$_{arom}$), 33.5 (m, P*C*HMe$_2$), 32.1 (m, P*C*HMe$_2$), 30.5 (m, P*C*HMe$_2$), 20.7 (PCH*Me*$_2$), 20.3 (PCH*Me*$_2$), 20.0 (PCH*Me*$_2$), 19.2 (PCH*Me*$_2$), 19.0 (PCH*Me*$_2$), 18.6 (PCH*Me*$_2$), 14.4 (br, B*C*H$_2$P). ^{31}P{^{1}H} NMR (162 MHz, benzene-d_6): δ 53.34 (dt, 1 P, [PhBP$_3$′] *trans* to CO, $^1J_{PRh}$ = 92 Hz, $^2J_{PPcis}$ = 29 Hz), 36.58 (dd, [PhBP$_3$′] cis to CO, $^1J_{PRh}$ = 78 Hz, $^2J_{PPcis}$ = 29 Hz). ^{11}B NMR (160.46 MHz, benzene-d_6): δ −12.97. IR (cm^{-1}): 2017 (RhCO), 1983 (RhH), 1950 (RhH). Anal. Calcd for $C_{28}H_{55}OBP_3Rh$: C, 54.74; H, 9.02. Found: C, 54.55; H, 9.17.

X-ray Structure Determinations. Single-crystal X-ray diffraction data were collected from samples mounted on a quartz fiber using Paratone N hydrocarbon oil. Data collection was carried out using graphite-monochromated Mo Kα (λ = 0.71069 Å) radiation on a Siemens SMART diffractometer equipped with a CCD area detector. The preliminary orientation matrix and unit cell parameters were determined by collecting 60 10-s frames, followed by spot integration and least-squares refinement. A hemisphere of data was collected using ω scans of 0.3° counted for a total of 30, 20, 10, 20, 30, and 15 s per frame for **5**, **7**·(C$_7$H$_8$)$_{0.5}$, **11**, **12**, **13**, and **14**, respectively. The frame data were integrated using the program SAINT (SAX Area-Detector Integration Program; V4.024; Siemens Industrial Automation, Inc.: Madison, WI, 1995). The program SADABS (Siemens Area Detector Absorption Corrections; Sheldrick, G. M., 1996) was utilized for scaling of diffraction data and the application of an empirical absorption correction based on redundant reflections. With the exception of **13**, the structures were solved using the teXsan crystallographic software package of the Molecular Structure Corp. using direct methods, and expanded with Fourier techniques. The function minimized in the full-matrix least-squares refinement was $\sum w(|F_o| - |F_c|)^2$. In the case of **13**, the structure was solved using the direct methods procedure in the Siemens SHELXTL (Sheldrick, G. M., Version 5.03;

Table 8. Crystallographic Data for Compounds 5, 7·$(C_7H_8)_{0.5}$, 11, 12, and 14

	5	7·$(C_7H_8)_{0.5}$	11	12	14
empirical formula	$IrP_3SiC_{31}H_{58}B$	$IrP_4C_{33.5}H_{64}B$	$RhP_3C_{29}H_{53}O_2B$	$RhP_3C_{27}H_{53}B$	$RhP_3SiC_{35}H_{57}B$
fw	754.84	793.80	640.37	584.35	712.56
cryst color, habit	off-white, plate	pale yellow, plate	yellow, plate	red-orange, plate	pale yellow, plate
cryst size (mm)	0.24 × 0.17 × 0.03	0.28 × 0.15 × 0.07	0.25 × 0.20 × 0.14	0.29 × 0.27 × 0.05	0.25 × 0.15 × 0.06
cryst syst	triclinic	monoclinic	monoclinic	monoclinic	triclinic
space group	$P\bar{1}$(#2)	$C2/c$ (#15)	$P21/a$ (#14)	$P21/n$ (#14)	$P\bar{1}$ (#2)
a (Å)	10.1906(6)	36.527(3)	15.5038(8)	9.2758(5)	9.3582(6)
b (Å)	12.8762(8)	10.0508(7)	11.4661(6)	11.9315(7)	11.1131(7)
c (Å)	14.0826(9)	20.125(1)	18.013(1)	27.907(2)	18.206(1)
α (deg)	88.929(1)	90	90	90	86.251(1)
β (deg)	75.703(1)	92.273(2)	92.326	99.149(1)(2)	86.214(1)
γ (deg)	87.422(1)	90	90	90	79.474(1)
V (Å^3)	1788.8(2)	7382.7(8)	3199.5(3)	3049.3(3)	1854.7(2)
no. of orientation reflns (2θ range)	5064 (3.5−45°)	5346 (3.5−45°)	6743 (3.5−45°)	5633 (3.5−45°)	4218 (3.5−45°)
Z value	2	8	4	4	2
D_{calc} (g/cm^3)	1.401	1.428	1.329	1.273	1.276
F_{000}	770.00	3256.00	1352.00	1240.00	752.00
μ (Mo Kα) (cm^{-1})	39.28	38.21	7.06	7.29	6.43
diffractometer	SMART	SMART	SMART	SMART	SMART
radiation	Mo Kα (λ = 0.71069 Å) graphite monochromated				
temperature (°C)	−149	−149	−130	−139	−99
scan type	ω (0.3° per frame)				
scan rate (s)	30	20	10	20	15
$2\theta_{max}$ (deg)	49.5	49.5	49.4	49.4	49.5
no. reflns measd	total: 8949 unique: 5673	total: 18 547 unique: 6559	total: 14 194 unique: 5588	total: 14 738 unique: 5260	total: 9265 unique: 5864
R_{int}	0.035	0.049	0.038	0.074	0.040
transmn factors	T_{min}/T_{max} = 0.42	T_{min}/T_{max} = 0.46	T_{min}/T_{max} = 0.62	T_{min}/T_{max} = 0.43	T_{min}/T_{max} = 0.23
structure solution	direct methods (SIR92)				
refinement method	full-matrix least-squares on F				
no. of observations	4553	4918	4065	2659	4344
no. of variables	331	354	320	290	365
reflns/param ratio	13.76	13.89	12.70	9.17	11.90
residuals: R; R_w; R_{all}	0.041; 0.048; 0.053	0.030; 0.039; 0.039	0.030; 0.037; 0.042	0.041; 0.048; 0.077	0.049; 0.060; 0.068
goodness of fit	1.34	1.13	1.12	1.08	1.45
max. shift/error in final cycle	0.00	0.00	0.00	0.00	0.00
max. and min. peaks in final diff map (e$^-$/Å^3)	1.50, −2.13	1.11, −1.70	0.63, −0.94	0.79, −1.17	1.20, −1.70

Table 9. Crystallographic Data for Compound 13

empirical formula	$RhP_4C_{30}H_{62}B$	radiation	Mo Kα (λ = 0.71069 Å)
fw	660.40		graphite monochromated
cryst color, habit	yellow, block	scan type	ω (0.3° per frame)
cryst size (mm)	0.11 × 0.10 × 0.08	scan rate	30 s
cryst syst	monoclinic	$2\theta_{max}$ (deg)	48.08
space group	$P2_1/c$ (#14)	no. reflns measd	total: 14147
a (Å)	10.993(2)		unique: 5047
b (Å)	16.887(3)	R_{int}	0.086
c (Å)	18.951(4)	transmn factors	T_{min}/T_{max} = 0.48
α (deg)	90	refinement method	full-matrix least-squares on F^2
β (deg)	90.96(3)	structure solution	direct methods (SHELXS-86)
γ (deg)	90	no. of observations	4044
V (Å^3)	3517.6(12)	no. of variables	320
no. of orientation reflns (θ range)	2800 (3.5−45°)	reflns/param ratio	12.64
Z value	4	final R indices ($I > 2\sigma(I)$)	R1 = 0.0604, wR2 = 0.1414
D_{calc} (g/cm^3)	1.247	R indices (all data)	R1 = 0.1085, wR2 = 0.1655
F_{000}	1408.00	goodness of fit	1.12
μ(Mo Kα) (cm^{-1})	6.85	max. shift/error in final cycle	0.00
diffractometer	SMART	max. and min. peaks in final diff map (e$^-$/Å^3)	1.452, −0.792
temperature (°C)	−143		

Siemens Crystallographic Research Systems: Madison, WI, 1994) program library, and refinement was carried out using the full-matrix least-squares method on F^2. Apart from noted exceptions, non-hydrogen atoms were refined anisotropically, with the exception of boron, which was refined isotropically. Unless otherwise noted, hydrogen atoms were included in calculated positions but not refined. The weighting scheme was based on counting statistics and included a p-factor to down-weight the intense reflections. Selected crystal and structure refinement data are summarized in Tables 8 and 9.

For 5. Crystals suitable for X-ray diffraction were obtained from a diethyl ether solution at room temperature. The Si atom of the $SiHEt_2$ ligand was found to be disordered over two positions (Si(1) and Si(2)). Si(1) was refined anisotropically with 70% occupancy, while Si(2) was refined isotropically with 30% occupancy. Additionally, the ethyl group comprised of C(3)

and C(4) was found to be disordered, exhibiting an alternate orientation (C(32) and C(33)). C(3), C(4), C(32), and C(33) were refined isotropically, with C(3) and C(4) at 70% occupancy, while C(32) and C(33) were assigned 30% occupancy. All remaining non-hydrogen atoms were refined anisotropically, with the exception of the boron atom, B1, which was refined isotropically. All carbon-bound hydrogen atoms were included in geometrically calculated positions and not refined.

For 7·$(C_7H_8)_{0.5}$. Crystals suitable for X-ray diffraction were obtained from a toluene solution at −30 °C. The structure was found to contain one molecule of the iridium complex and half of a toluene molecule per asymmetric unit. The toluene molecule is disordered over two positions that are related by a crystallographically imposed mirror plane and was modeled as seven half-occupancy carbon atoms (C31−C37), which were refined isotropically. All remaining non-hydrogen atoms were refined anisotropically, with the exception of the boron atom, B1, which was refined isotropically. All hydrogen atoms were included in geometrically calculated positions and not refined, with the exception of H1 and H2, which were located in the difference Fourier map and their positional coordinates were refined.

For 11. Crystals suitable for X-ray diffraction were obtained from a diethyl ether solution at −30 °C. The structure was found to contain one molecule of the rhodium complex per asymmetric unit. All non-hydrogen atoms were refined anisotropically, with the exception of the boron atom, B1, which was refined isotropically. All hydrogen atoms were included in geometrically calculated positions and not refined.

For 12. Crystals suitable for X-ray diffraction were obtained from a diethyl ether solution at −30 °C. The structure was found to contain one molecule of the rhodium complex per asymmetric unit. All non-hydrogen atoms were refined anisotropically, with the exception of the boron atom, B1, which was refined isotropically. All hydrogen atoms were included in geometrically calculated positions and not refined, with the exception of H1 and H2, which were located in the difference Fourier map and their positional coordinates were refined.

For 13. Crystals suitable for X-ray diffraction were obtained from a toluene solution at −30 °C. The structure was found to contain one molecule of the rhodium complex per asymmetric unit. All non-hydrogen atoms were refined anisotropically, with the exception of the boron atom, B1, which was refined isotropically. All carbon-bound hydrogen atoms were included in geometrically calculated positions and not refined.

For 14. Crystals suitable for X-ray diffraction were obtained from a diethyl ether solution at −30 °C. The structure was found to contain one molecule of the rhodium complex per asymmetric unit. All non-hydrogen atoms were refined anisotropically, with the exception of the boron atom, B1, which was refined isotropically. All carbon-bound hydrogen atoms were included in geometrically calculated positions and not refined, with the exception of H1, which was located in the difference Fourier map and its positional coordinates were refined.

Acknowledgment is made to the National Science Foundation for their generous support of this work. We thank Dr. Frederick J. Hollander and Dr. Allen G. Oliver for assistance with the X-ray structure determinations.

Supporting Information Available: Summaries of crystallographic data, bond distances and angles, atomic coordinates, and anisotropic displacement parameters for **5**, **7**·$(C_7H_8)_{0.5}$, **11**, **12**, **13**, and **14**. This material is available free of charge via the Internet at http://pubs.acs.org.

OM030686E